Intrasubject subcortical quantitative referencing to boost MRI sensitivity to Parkinson's disease

Laila Khedher, Jean-Marie Bonny, Ana Marques, Elodie Durand, Bruno Pereira, Marie Chupin, Tiphaine Vidal, Carine Chassain, Luc Defebvre, Nicolas Carriere, et al.

HAL Id: hal-03857470
https://hal.inrae.fr/hal-03857470v1

Submitted on 1 Oct 2024

Intrasubject subcortical quantitative referencing to boost MRI sensitivity to Parkinson's disease

Laila Khedher [a,d,*], Jean-Marie Bonny [b,d], Ana Marques [a,c], Elodie Durand [a,c], Bruno Pereira [e], Marie Chupin [f], Tiphaine Vidal [a,c], Carine Chassain [a,c], Luc Defebvre [g], Nicolas Carriere [g], Valerie Fraix [h], Elena Moro [h], Stéphane Thobois [i,j,k], Elise Metereau [i,j,k], Graziella Mangone [l], Marie Vidailhet [l], Jean-Christophe Corvol [l], Stéphane Lehéricy [l], Nicolas Menjot de Champfleur [m,n], Christian Geny [o,p], Umberto Spampinato [q], Wassilios Meissner [q,r,s], Solène Frismand [t], Emmanuelle Schmitt [t], Anne Doé de Maindreville [u], Christophe Portefaix [v,w], Philippe Remy [x], Gilles Fénelon [x], Jean Luc Houeto [y], Olivier Colin [z], Olivier Rascol [aa], Patrice Peran [aa], Franck Durif [a,c], and the R study group[1]

[a] University Clermont Auvergne, CNRS, Clermont Auvergne INP, Institut Pascal, Clermont-Ferrand, France
[d] AgroResonance, INRAE, 2018. Nuclear Magnetic Resonance Facility for Agronomy, Food and Health, doi: 10.15454/1.5572398324758228E12, France
[b] AgroResonance UR370 QuaPA - INRAE, Saint-Genès-Champanelle 63122, France
[c] Clermont-Ferrand University Hospital, Neurology Department and NS-PARK/FCRIN Network, Clermont-Ferrand, France
[e] Clermont-Ferrand University Hospital, Biostatistics Unit (DRCI), Clermont-Ferrand, France
[f] Sorbonne Université, Institut du Cerveau - ICM, CATI, Assistance Publique Hôpitaux de Paris, Inserm, CNRS, Département de Neurologie and NS-PARK/FCRIN Network, CIC Neurosciences, Hôpital Pitié-Salpêtrière, Paris, France
[g] Department of Movement Disorder and NS-PARK/FCRIN Network, Inserm 1172 University of Lille, Lille, France
[h] Service de Neurologie, CHU de Grenoble and NS-PARK/FCRIN Network, Université Grenoble Alpes, Grenoble Institute of Neuroscience, Grenoble, France
[i] CNRS, Institut des Sciences Cognitives Marc Jeannerod, UMR 5229 CNRS, Lyon, France
[j] Université Claude Bernard, Lyon I, Lyon, France
[k] Hospices Civils de Lyon, Hôpital Neurologique Pierre Wertheimer, Service de Neurologie C and NS-PARK/FCRIN Network, Lyon, France
[l] Sorbonne Université, Institut du Cerveau - ICM, Assistance Publique Hôpitaux de Paris, Inserm, CNRS, Département de Neurologie and NS-PARK/FCRIN Network, CIC Neurosciences, Hôpital Pitié-Salpêtrière, Paris, France
[m] Department of Neuroradiology, Montpellier University Hospital Center, Gui de Chauliac Hospital, Montpellier, France
[n] I2FH, Institut d'Imagerie Fonctionnelle Humaine, Hôpital Gui de Chauliac, CHRU de Montpellier, Montpellier, France
[o] Department of Geriatrics and NS-PARK/FCRIN Network, Montpellier University Hospital, Montpellier University, Montpellier, France
[p] EuroMov Laboratory, University of Montpellier, 700 Avenue du Pic Saint Loup, Montpellier, Montpellier 34090, France
[q] Service de Neurologie - Maladies Neurodégénératives and NS-PARK/FCRIN Network, CHU Bordeaux, Bordeaux F-33000, France
[r] Univ. Bordeaux, CNRS, IMN, UMR 5293, Bordeaux, Bordeaux F-33000, France
[s] Dept. Medicine, University of Otago, Christchurch, and New Zealand Brain Research Institute, Christchurch, New Zealand
[t] Service de Neurologie and NS-PARK/FCRIN Network, CHRU-Nancy, Nancy, France
[u] Department of Neurology and NS-PARK/FCRIN Network, Hôpital Maison blanche, Reims, France
[v] Department of Radiology, Hôpital Maison blanche, Reims, France
[w] CReSTIC Laboratory (EA 3804), University of Reims Champagne-Ardenne, Reims, France
[x] Centre Expert Parkinson and NS-PARK/FCRIN Network, CHU Henri Mondor, AP-HP et Equipe Neuropsychologie Interventionnelle, INSERM-IMRB, Faculté de Santé, Université Paris-Est Créteil et Ecole Normale Supérieure Paris Sorbonne Université, Créteil, France
[y] INSERM, CHU de Poitiers, Université de Poitiers, Centre d'Investigation Clinique CIC1402, Service de Neurologie and NS-PARK/FCRIN Network, Poitiers, France – CHU - Centre Expert Parkinson de Limoges, Limoges, France

[z] INSERM, CHU de Poitiers, Université de Poitiers, Centre d'Investigation Clinique CIC1402, Service de Neurologie and NS-PARK/FCRIN Network, Poitiers, France– CH Brive la Gaillarde, France
[aa] Centre d'Investigation Clinique CIC 1436, UMR 1214 TONIC and NS-PARK/FCRIN Network, INSERM, CHU de Toulouse et Université de Toulouse3, Toulouse, France

ARTICLE INFO

ABSTRACT

Several postmortem studies have shown iron accumulation in the substantia nigra of Parkinson's disease patients. Iron concentration can be estimated via MRI-R_2^* mapping. To assess the changes in R_2^* occurring in Parkinson's disease patients compared to controls, a multicentre transversal study was carried out on a large cohort of Parkinson's disease patients (n = 163) with matched controls (n = 82). In this study, 44 patients and 11 controls were removed due to motion artefacts, 21 patient and 6 controls to preserve matching. Thus, 98 patients and 65 age and sex-matched healthy subjects were selected with enough image quality.

The study was conducted on patients with early to late stage Parkinson's disease. The images were acquired at 3Tesla in 12 clinical centres. R_2^* values were measured in subcortical regions of interest (substantia nigra, red nucleus, striatum, globus pallidus externus and globus pallidus internus) contralateral (dominant side) and ipsilateral (non dominant side) to the most clinically affected hemibody.

As the observed inter-subject R_2^* variability was significantly higher than the disease effect, an original strategy (intrasubject subcortical quantitative referencing, ISQR) was developed using the measurement of R_2^* in the red nucleus as an intra-subject reference.

R_2^* values significantly increased in Parkinson's disease patients when compared with controls; in the substantia nigra (SN) in the dominant side (D) and in the non dominant side (ND), respectively (P_{SN_D} and $P_{SN\_ND} <$ 0.0001). After stratification into four subgroups according to the disease duration, no significant R_2^* difference was found in all regions of interest when comparing Parkinson's disease subgroups.

By applying our ISQR strategy, $R_{2(ISQR)}^*$ values significantly increased in the substantia nigra (P_{SN_D} and $P_{SN\_ND} <$ 0.0001) when comparing all Parkinson's disease patients to controls.

$R_{2(ISQR)}^*$ values in the substantia nigra significantly increased with the disease duration ($P_{SN\_D} = 0.01$; $P_{SN\_ND} = 0.03$) as well as the severity of the disease (Hoehn & Yahr scale <2 and ≥ 2, $P_{SN\_D} = 0.02$). Additionally, correlations between $R_{2(ISQR)}^*$ and clinical features, mainly related to the severity of the disease, were found.

Our results support the use of ISQR to reduce variations not directly related to Parkinson's disease, supporting the concept that ISQR strategy is useful for the evaluation of Parkinson's disease.

1. Introduction

Post mortem histological analysis (Dexter et al., 1989; Riederer et al., 1989), showed the concentration of iron increasing from 30 to 100 % in the substantia nigra of Parkinson's disease patients compared to controls. However, results are controversial in other basal ganglia structures (Wei and Wang, 2016). At the pathophysiological level, the overload of iron storage in the substantia nigra exaggerates oxidative stress, accelerates aggregation of alpha-synuclein (Wolozin and Golts, 2002) and could lead to cell damage.

MRI relaxometry is a powerful tool used to detect iron deposits in the brain as its paramagnetism induces magnetic field inhomogeneities that accelerate relaxation rates (Tosk et al., 1992; Brooks et al., 1989; Schenck, 1995). In vivo (Gelman et al., 1999) and post mortem (Langkammer et al., 2010) studies converged in showing that both R_2 and R_2' transverse relaxation rates are influenced by the presence of iron in the brain. R_2 and R_2' are both linearly and positively correlated with iron concentration, with roughly similar respective slopes. Because R_2^* is made up of the sum of these two irreversible (R_2) and reversible (R_2') components, R_2^* is thus more sensitive to iron content. In addition, R_2^* can be easily mapped in the brain by using magnitude of gradient recalled echo images at multiple echo times (Chavhan et al., 2009).

R_2^* variations due to Parkinson's disease have been extensively studied in vivo. With rare exceptions (Liu et al., 2019; Reimão et al., 2015), most of the studies have demonstrated higher R_2^* in the substantia nigra of Parkinson's disease patients (Barbosa et al., 2015; Baudrexel et al., 2010; Du et al., 2018; Du et al., 2011; Graham et al., 2000; Guan et al., 2017; Hopes et al., 2016; Langkammer et al., 2016; Langley et al.,

2017; Lewis et al., 2013; Martin and Gee, 2008; Péran et al., 2010; Ulla et al., 2013; Wallis et al., 2008). In basal ganglia (caudate nucleus, putamen, globus pallidus), recent studies found no change of R_2^* (Barbosa et al., 2015; Baudrexel et al., 2010; Guan et al., 2017; Hopes et al., 2016; Langkammer et al., 2016; Martin and Gee, 2008; Péran et al., 2010). If elevated iron levels could lead to dopaminergic neuron denervation in the substantia nigra of Parkinson's disease patients, links between R_2^* values and clinical characteristics of patients with Parkinson's disease such as disease duration and severity should be observed. In fact, although longitudinal studies have confirmed that variation in R_2^* may capture Parkinson's disease-related progression in the substantia nigra (Du et al., 2018; Hopes et al., 2016; Ulla et al., 2013), others failed to detect a longitudinal change (Arribarat et al., 2019; Wieler et al., 2015) or showed that rather than correlating with disease duration, the rate of change was associated with individual characteristics, such as cognitive decline and age in later stages of Parkinson's disease (Rossi et al., 2014). Looking at the data in the literature, R_2^* is not considered to be very sensitive as an indicator of disease progression.

The strategy implemented by these studies was the search for a mean group effect which implicitly neglects the inter-subject variability by treating it as noise. However, when reported, the between-subject standard deviation of R_2^* in substantia nigra was between 15 and 20 %, in patients as well as controls. Such high variability of R_2^* could limit the use of this parameter as a surrogate biomarker in order to track the progression of Parkinson's disease.

Several factors can explain such inter-subject variability; (i) the biological heterogeneity of parkinsonian patients, e.g. the large range of age (47 to 72 years) and duration of disease (1–13 years) (Pyatigorskaya et al., 2020), (ii) positioning errors when defining the substantia nigra region which differ according to the segmentation techniques used (e.g. manual or automatic), (iii) differences in measurement conditions

---

[1] Collaborators in the R* study are listed in the Appendix.

which cannot be strictly standardized from one subject to another, e.g. orientation of the head in the coil, (iv) the structural factors contributing to the subtle magnetic properties of the brain which thus may change R_2^* of the substantia nigra independently from the disease, e.g. the surrounding myelin (Duyn, 2017).

The role of this cross-sectional study is to clarify how much R_2^* is changing as a function of the disease stage while tackling several of the issues that arise due to inter-subject variability. First, it was designed to measure R_2^* values in subcortical regions of interest (substantia nigra, red nucleus, striatum, globus pallidus externus and globus pallidus internus) contralateral (dominant side) and ipsilateral (non dominant side) to the most clinically affected hemibody, in four groups of patients from early to late stages of the disease and matched controls. Clinical data assessing motor and non-motor signs was assessed to measure the severity of the disease. In addition, a new intra-subject referencing technique was introduced in order to isolate the variation of R_2^* associated with Parkinson's disease from other sources of R_2^* variance.

2. Materials and methods

2.1. Study subjects

This study was an ancillary part of the IPD-R_2^* study which is an ongoing multicentre prospective study of Parkinson's disease patients assessing the amount of iron in the brain by MRI. Patients were recruited between August 2015 – June 2019 by 12 French University hospitals of the French national NS-Park/FCRIN network (https://www.parkinson.network/).

The protocol was approved by the research ethical committee (Comité de Protection des Personnes, AU1135, France). All participants gave written informed consent. The study was registered on the clinicaltrials.gov website (Ref. Clinical Trial = NCT02816645). Inclusion criteria was diagnosis of Parkinson's disease according to MDS clinical criteria for Parkinson's disease (Postuma et al., 2015). Exclusion criteria were severe cognitive impairment (Montreal Cognitive Assessment (MoCA) < 24) (Nasreddine et al., 2005) and atypical parkinsonism. Clinical data were collected at baseline, and one year later. MRI was performed at the baseline visit and then one year later to evaluate variations of volume structures, diffusion parameters, and iron content. Here, only clinical and R_2^* measurements from MRI data obtained at baseline were used.

2.2. Study design and clinical scores

Patients were selected according to duration of disease (Group1 (G1) < 5 years, Group2 (G2) ≥ 5 and < 10 years, Group3 (G3) ≥ 10 and < 15 years and Group4 (G4) ≥ 15 years) with the aim of recruiting 40 patients per subgroup. Control subjects were matched for each subgroup according to age (±5 years) and sex.

Clinical assessments at baseline included collection of demographic data, medical and treatment history. Parkinsonism evaluation was assessed using the Movement Disorder Society-Unified Parkinson's Disease Rating Scale (MDS-UPDRS) parts I-IV (Goetz et al., 2008) which assesses non-motor and motor experiences of daily living (MDS-UPDRS I, II), motor examination (MDS-UPRDS III) and motor complications (MDS-UPDRS IV), the Hoehn & Yahr (H&Y) scale (Hoehn and Yahr, 1998), the Schwab & England (S&E) scale (Schwab, 1960) and the Freezing of Gait Questionnaire (FOG-Q) (Giladi et al., 2009). To determine the most affected hemibody, the sum of the following MDS-UPRDS III items were calculated for the left and right hemibody: rigidity, finger tapping, hand movements; pronation-supination movements of hands; toe tapping; leg agility, postural and kinetic tremor of the hands; rest tremor amplitude for upper and lower limbs. The body side with the higher score for these items was considered as the dominant side. In addition, a neuropsychological assessment was performed, using a MoCA for global efficiency, the Lille Apathy Rating Scale (LARS)

(Sockeel et al., 2006), the Hamilton Rating Scale for Depression (HAM-D) (Hedlund and Vieweg, 1979) and the Hamilton Rating Scale for Anxiety (HAM-A) (Hamilton, 1959). Regarding psycho-behavioral symptoms, the French version of Ardouin Scale of Behavior in Parkinson's Disease (ASBPD) was used to assess hypo and hyperdopaminergic disorders, non-motor fluctuations and impulse-control disorders (ICD) (compulsive eating, hobbyism, punding, compulsive shopping, pathological gambling, hypersexuality, dopaminergic addiction) (Rieu et al., 2015). Finally, self-questionnaires were completed, including the Epworth Sleepiness Scale (ESS) (Johns, 1991), the assessment of Autonomic Dysfunction in Parkinson's Disease (SCOPA-AUT) (Visser et al., 2004) and Non-Motor Symptom assessment Scale for Parkinson's Disease (NMSS) (Chaudhuri et al., 2006). The Levodopa Equivalent Daily Dose (LEDD) was provided for each patient taking into account levodopa treatments, dopamine agonists, and other antiparkinsonian drugs such as MAO-B inhibitors, COMT inhibitors and amantadine (Tomlinson et al., 2010). Regarding healthy control subjects, the LARS, HAM-A and HAM-D were performed in addition to the MoCA. A maximum of ± 3 months was allowed between clinical evaluations and MRI acquisition.

2.3. MRI data acquisition

MRI was performed at 3T by 12 French clinical centres with different magnetic resonance imaging scanners. Sixty-six patients with Parkinson's disease and 32 healthy controls were scanned with a General Electric MRI scanner (GE Healthcare, Waukesha, WI, USA), 35 Parkinson's disease patients and 14 healthy controls with a Philips MRI scanner (Philips, Best, Netherlands), 62 Parkinson's disease patients and 36 healthy controls subjects with a Siemens MRI scanner (Siemens, Erlangen, Germany) (see Supplementary Information Table, Table 1).

The implementation of the MRI protocol at the 12 centres was carried out in collaboration with the CATI platform (Centre for Image Acquisition and Processing, Neurospin, CEA, Saclay, France, https://cati-neuroimaging.com). All MRI systems used identical three-dimensional (3D) multiple GRE sequences with matching parameters, in order to limit inter-site variability. The protocol was designed to obtain images in less than ten minutes in order to reduce the effect of head movement (Gay et al., 2016). Datasets were acquired on the NIST test-object (Russek et al., 2012) to confirm the between-centre consistency of the R_2^* measurement. Protocol consistency monitoring and quality control was ensured by CATI for the duration of the study.

All subjects were equipped with a multichannel receive-only array head coil and were immobilized by foam pads during acquisition to reduce involuntary head movements. Disposable ear plugs were also used to reduce acoustic noise. The sequence parameters were as follows: field of view $256 \times 256 \times 160$ mm^3, leading to a voxel volume of $1 \times 1 \times 1$ mm^3; 6 equidistant echo times (TE = 4.28, 9.54, 14.79, 20.05, 25.31, 30.56 ms). The duration of the 3D multiple GRE sequence was about 10 min.

Acquired datasets were evaluated regarding their reliability for further analyses and divided into three categories: reject, borderline and OK. The quality control for 3D multi GRE sequences was based on a systematic procedure, to try to minimise subjective assessment. Relative uncertainty maps were computed together with R2* single exponential maps. Mean values were computed in regions coregistered from the AAL atlas (lentiform nuclei and thalami) to give a first estimate of measurement reliability, by comparing the values to thresholds previously estimated on another database. However, local values only give information on the underlying area. These values were thus confirmed by a systematic overall visual evaluation on the first, third and fifth echoes, together with the R2* and uncertainty maps displayed with predefined ranges and colormaps, to rate specific artefacts according to a three point grade, mainly wrinkles due to motion, blur due to motion, artefacts localised in the area of interest, artefacts due to eye motion and artefacts due to susceptibility (0 meaning no visible artefact, 1

indicating an artefact but the underlying structure is still well defined and 2 indicating that the underlying borders are no longer correctly defined because of the artefact). A global qualitative index and a final decision are then inferred from these items, thus giving a more objective basis to this rating.

Data of lower quality were excluded from analysis (reject category).

2.4. MRI data processing and analysis

2.4.1. R_2^* mapping

The six magnitude GRE images for each participant were spatially normalized using standard SPM12 procedures (Statistical Parametric Mapping, Wellcome Department of Cognitive Neurology, London, UK). To correct for any between-echo misregistration, the images were linearly registered to the first TE image using the SPM tool REALIGN in order to estimate and apply a rigid-body affine transformation with 6 degrees of freedom and cubic spline interpolation. Then, to segment into grey matter, white matter and CSF probability maps, the first echo of

2.4.3. Intrasubject subcortical quantitative referencing (ISQR)

In our study, the R_2^* inter-subject variability (i.e. the relative standard deviation of R_2^* within the considered group) obtained both in Parkinson's disease patients and controls was substantial, between 10 and 20 %. This variability was mostly independent of the disease (see results and the discussion). In order to remove this non-specific variability (i.e. between-subject R_2^* variation independent of the disease), the red nucleus was chosen as a reference structure for the following four reasons: (i) the red nucleus is not directly involved in the pathophysiology of Parkinson's disease (ii) no significant difference in R_2^* was found between patients and control subjects in this region (Table 2) (iii) the values of R_2^* in the red nucleus were close to those observed in the basal ganglia and specifically in the substantia nigra (Table 2) and (iv) R_2^* in the red nucleus and in the substantia nigra were correlated for control subjects (red nucleus = RN; $r_{SN\_D, RN\_D} = 0.56$, $P_{SN\_D, RN\_D} < 0.001$, $r_{SN\_ND, RN\_ND} = 0.49$, $P_{SN\_ND, RN\_ND} < 0.001$). Therefore, in addition to considering the raw value of R_2^* averaged in the different

$$R_{2(ISQR)}^*(\text{region of interest, subject}) = R_2^*(\text{region of interest, subject}) - R_2^*(\text{red nucleus, subject})$$

each subject image was used, utilizing the "new segment" approach (Ashburner and Friston, 2005). Lastly, the DARTEL pipeline was used for spatial normalization in which a study specific group template is created using an iterative process (Ashburner, 2007). The obtained subject-specific deformation fields were then applied to normalize the six TE images to the standard MNI space. This preprocessing step was only based on the multi-TE acquisitions and did not require further anatomical MRI, which reduced the risk of residual misregistration. Because the DARTEL pipeline is inherently a group-level procedure, all subjects belonging to a given group were spatially-normalized together. Hence, the DARTEL was applied to the four Parkinson's disease sub-groups and the four control groups separately.

For R_2^* mapping, these registered and spatially-normalized GRE images were non-linearly fitted voxel wise in the least-squares sense with a mono-exponential model as a function of TEs using an in-house MATLAB script (LSQNONLIN function). Hence the R_2^* maps were *de facto* obtained by the MNI reference space.

2.4.2. Regions of interest

10287005360670000Regions of interest were defined according the freely available ATAG probabilistic atlas (Keuken, 2014; Keuken and Bu, 2015). Five basal ganglia structures were selected: the substantia nigra, the red nucleus, the striatum, the globus pallidus externus and the globus pallidus internus. The degrees of membership were limited to 0.70 so as to fit to the structures and in particular to the SN (cf. Supplementary Fig. 1). R_2^* values were measured in the dominant and non-dominant sides in each brain structure. Grey matter and white matter regions were obtained from the previous segmentation step (new segment) using thresholding at $P = 0.95$.

To validate our automatic segmentation, the substantia nigra was also contoured manually on images of thirty control subjects. The manual contouring was performed by an expert neurologist in the field (F.D.). The manual segmentation was based on a single T_2^*-weighted image (GRE at TE = 25.3 ms) according to the previously described methods (Eapen et al., 2011) and a MRI atlas of the mesencephalon (Duvernoy, 1995) using ITK-SNAP (www.itksnap.org) (Yushkevich et al., 2006). A significant R_2^* correlation between automatic and manual contouring in controls was shown (substantia nigra = SN; $r_{SN\_D} = 0.73$, $r_{SN\_ND} = 0.76$ and both $P < 0.01$).

anatomical regions, we also considered the difference between this value and the one measured on the red nucleus, i.e.

The rationale of ISQR considers ferritin, which is mainly located within the subcortical nuclei, and neuromelanin, which is more specific of dopaminergic neurons in the SN, are two independent compartments. These field creating objects thus act on the T2 relaxation as two multiplicative mono-exponential decays which give rise to a total apparent decay in which the relaxation rates of the two compartments add. Following these assumptions, subtracting the R_2^* value of the red nucleus is a natural operation for removing the influence of individual variation independent of the disease.

2.5. Statistical analysis

Sample size was calculated according to (i) Cohen's recommendations (Cohen, 1988) which define effect-size bounds as small (ES: 0.2), medium (ES: 0.5) and large (ES: 0.8, "grossly perceptible and therefore large") and (ii) to the work of Marek et al. (Marek et al., 2011), in which for every-two patients, at least one control participant was included.

Continuous data were expressed as mean and standard-deviation or median and interquartile range, according to statistical distribution. The assumption of normality was assessed using the Shapiro-Wilk test. The comparisons between groups (i.e. between disease duration sub-groups) were performed using linear mixed model taking into account centre and machine effects (as random-effects), and when appropriate, pairing effect for patient vs control subject comparisons. The normality of residuals from these models was studied using the Shapiro-Wilk test. When necessary, a logarithmic transformation was applied to achieve the normality of dependent outcomes. The results were expressed using Hedge's effects-size and were interpreted according to the aforementioned Cohen's rules of thumb. To take into account our multiple comparison study, a Sidak's type 1 error correction was applied. Then, multivariate analyses have been performed using adjustment on covariates fixed according to the univariate results and to the clinical relevance: HY, treatment, MDS-UPDRS part IV and quality of images. A particular attention was paid on multicollinearity of covariates. Effect-sizes were then compared according to disease duration by the analyze of interaction between PD and healthy subjects in multivariate analyses. The relationships between quantitative variables were

analyzed using correlation coefficients (Pearson or Spearman, according to the statistical distribution). The results were represented using a color heatmap. A Sidak's type I error correction was applied to take into account multiple comparisons.

Finally, discriminant factorial analysis was performed (i) to illustrate the relationship between clinical characteristics and R_2^* parameters using principal component analysis and then (ii) to highlight associations between R_2^* parameters and disease duration with discriminant analysis. These statistical methods were useful for analyzing assets as elements of quantitative variables in order to uncover the underlying relationships and structures of the variables measured (latent constructs) and to aggregate subjects into clusters such that each cluster represents a topic (i.e. disease duration).

Analyses were performed with Stata 15.0 (StataCorp, College Station, US) and software R (package ade4) for factorial analyses. The tests were two-sided, with a type I error set at 5 %.

3. Results

3.1. Demographic information

One hundred and sixty-three patients with Parkinson's disease and

82 age and sex-matched controls were recruited at baseline. Forty-four patients and 11 controls were excluded from the analysis after rejection of the 3D multiple GRE sequence during the CATI quality control procedure due to movements or the presence of artefacts, i.e. 27 % of patients and 14 % of controls. The exclusion of the other subjects (21 patients and 6 controls) is related to our desire to keep the matching between patients and controls. Thus, 98 Parkinson's disease patients (60 males and 38 females) and 65 age and sex-matched healthy subjects (35 males and 30 females) were selected with enough image quality, i.e. low noise and fewer artifacts (Fig. 1).

Table 1 summarizes the demographic and clinical characteristics of the subjects. Compared to controls, Parkinson's disease patients had significantly higher HAM-D scores ($P = 0.02$) and LARS-scores ($P = 0.001$). Moreover, a significant difference was observed between the Parkinson's disease subgroups according to disease duration and MDS-UPDRS IV ($P = 0.001$), FOG-Q ($P = 0.001$), H&Y ON ($P = 0.02$) and LEDD ($P = 0.001$). A significant difference was observed also when comparing MDS-UPDRS III ON_D. vs MDS-UPDRS III ON_ND in all Parkinson's disease patients and in each Parkinson's disease sub-groups (p < 0.001).
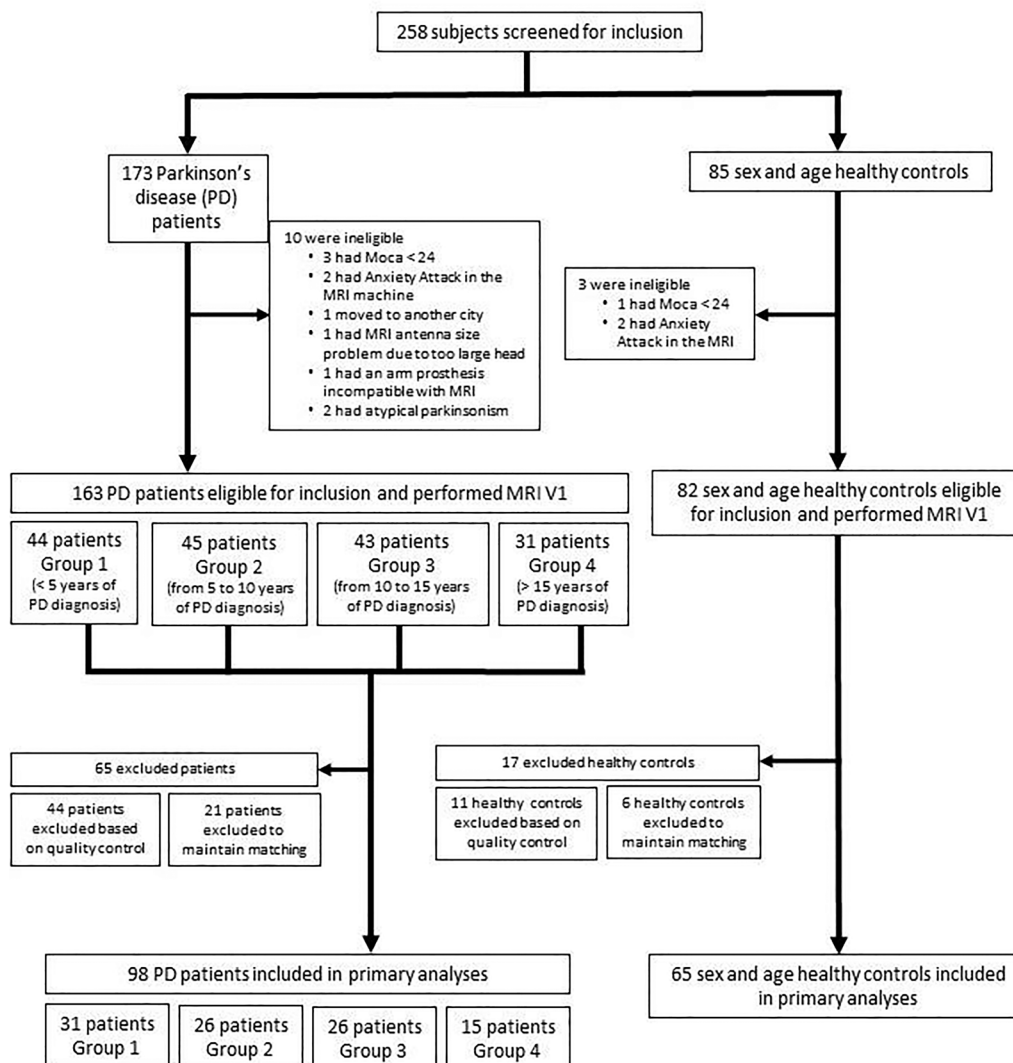
Fig. 1. Flow chart inclusion of study participants. 258 participants (173 patients with Parkinson's disease and 85 age and sex-matched controls) were recruited at baseline. An image quality analysis protocol was established in this study. This protocol allowed us to carry out our current study only on 98 Parkinson's disease patients (60 males and 38 females) and 65 age and sex-matched healthy subjects (35 males and 30 females). Parkinson's disease patients were stratified in four groups according to the duration of the disease (Group1 < 5 years; Group2 > 5 and < 10 years; Group3 > 10 and < 15 years and Group4 > 15 years).

Table 1
Demographic and clinical characteristics of subjects.

	All PD patients	Paired controls	PD patients G1	PD patients G2	PD patients G3	PD patients G4	P value
Number of subjects	98	65	31	26	26	15	
Age (years)	64.0 ± 7.7	64.2 ± 7.8	62.4 ± 9.1	63.6 ± 6.4	65.7 ± 7.6	65.2 ± 6.8	0.81 [a] 0.39 [b]
Sex (Male/Female)	60 (61 %) / 38 (39 %)	36 (55 %) / 30 (45 %)	19 (61 %) / 12 (39 %)	14 (54 %) / 12 (46 %)	14 (54 %) / 12 (46 %)	13 (87 %) / 2 (13 %)	Na
Disease duration (years)	8.1 ± 5.7	na	1.9 ± 1.5	6.7 ± 1.5	11.6 ± 1.6	17.1 ± 3.8	**< 0.001**[b]
MDS-UPDRS I score (/52)	9.4 ± 5.4	na	7.6 ± 5	9.7 ± 5.7	11.0 ± 4.7	10.2 ± 6.1	0.1 [b]
MDS-UPDRS II ON score (/52)	8.3 ± 5.7	na	7.3 ± 5.3	7.7 ± 5.4	9.4 ± 5.8	9.7 ± 6.7	0.4 [b]
MDS-UPDRS III ON score (/132)	19.0 ± 12.0	na	17.9 ± 11.3	15.9 ± 9.7	19.7 ± 13	25.4 ± 13.7	0.11[b]
MDS-UPDRS III ON _D	8.32 ± 4.7	na	9 ± 4.93	7.4 ± 3.73	7.88 ± 4.77	9.28 ± 5.66	**< 0.001**
MDS-UPDRS III ON _ND	4.33 ± 4.06	na	3.42 ± 3.73	3.52 ± 3.35	5 ± 4.2	6.64 ± 4.89	
MDS-UPDRS IV score (/24)	3.3 ± 3.7	na	0.5 ± 1.6	3.3 ± 3.7	4.3 ± 3.8	6.4 ± 3.7	**< 0.001**[b]
H&Y ON score (from stage 0 to stage 5)	1.8 ± 0.7	na	1.7 ± 0.6	1.5 ± 0.8	1.9 ± 0.8	2.2 ± 0.5	**0.02**[b]
SE ON score (from 0 % to 100 %)	91.5 ± 6.5	na	92.6 ± 5.8	91.9 ± 6.9	89.2 ± 6.4	92.2 ± 7.0	0.22[b]
FOG-Q score (/24)	4.8 ± 5.2	na	2.5 ± 4.0	4.1 ± 4.7	5.6 ± 4.6	9.6 ± 6.2	**< 0.001**[b]
MoCA score (/30)	27.7 ± 1.6	27.4 ± 1.9	28.0 ± 1.6	27.7 ± 1.5	27.9 ± 1.7	26.7 ± 1.6	0.33 [a] 0.06 [b]
ASBPD I&II score (/28)	2.1 ± 1.9	na	1.8 ± 1.5	2.4 ± 2.1	2.6 ± 2.2	1.4 ± 1.6	0.71[b]
ASBPD III score (/8)	0.5 ± 0.8	na	0.1 ± 0.5	0.5 ± 0.8	0.6 ± 0.9	0.7 ± 1.1	0.11[b]
ASBPD IV score (/48)	2.3 ± 2.7	na	2.0 ± 2.7	2.5 ± 2.8	2.8 ± 3.1	1.7 ± 1.7	0.65[b]
ASBPD TOTAL score (/84)	4.8 ± 3.8	na	3.9 ± 2.7	5.4 ± 4.1	5.9 ± 4.3	3.9 ± 4.0	0.26[b]
HAM-D score (/54)	3.8 ± 4.1	2.4 ± 3.7	3.5 ± 2.9	3.9 ± 4.1	4.7 ± 5.4	2.5 ± 3.3	**0.02** [a] 0.41[b]
HAM-A score (/56)	3.6 ± 3.8	3.0 ± 3.4	4.0 ± 3.0	3.2 ± 3.1	4.3 ± 5.5	2.3 ± 2.7	0.28 [a] 0.36[b]
LARS score (from −36 to 36)	−28.4 ± 6.7	3.0 ± 3.4	−29.4 ± 4.9	−28.1 ± 9.6	−28.1 ± 5.6	−27.5 ± 6.0	**< 0.001** [a] 0.79[b]
ESS score (/24)	9.3 ± 4.7	Na	8.3 ± 5.6	8.6 ± 4.6	11.0 ± 4.1	9.7 ± 3.2	0.15[b]
NMSS score (/30)	8.3 ± 5.7	Na	6.6 ± 4.2	7.9 ± 6.6	10.3 ± 6.8	9.1 ± 3.7	0.09[b]
SCOPA AUT Females (/69)	11.6 ± 8.4	Na	12.0 ± 9.5	9.2 ± 7.8	13.6 ± 8.7	11.5 ± 3.5	0.51[b]
SCOPA AUT Males (/69)	12.5 ± 8.4	Na	10.8 ± 5.7	13.3 ± 10.5	13.0 ± 9.1	13.3 ± 9.0	0.67[b]
LEDD (mg/j)	759 ± 469	Na	393 ± 269	753 ± 405	1008 ± 358	1151 ± 532	**< 0.001**[b]

Values are expressed as Mean ± standard deviation; PD = Parkinson's disease; na = not applicable. G1: Group1 < 5 years; G2: Group2 > 5 and ≤ 10 years; G3: Group3 > 10 and ≤ 15 years, G4: Group4 > 15 years.
c: Statistical significance in ALL PD patients, in G1, in G2, in G3 and in G4 when comparing MDS-UPDRS III ON_D. vs MDS-UPDRS III ON_ND.
[a] : Statistical significance between PD patients and healthy controls.
[b] : Statistical significance between the PD subgroups according to disease duration.

3.2. Machine/center effects

Our current study was carried out by 12 clinical centres, with a variety of MRI scanners (General Electric, Philips, and Siemens). No difference in R_2^* values in the SN between the machines (for healthy controls; PSN_D and PSN_ND = 0.13 and for PD patients; PSN_D = 0.62 and PSN_ND = 0.35) and the centres (for healthy controls; PSN_D and PSN_ND = 0.23 and for PD patients; PSN_D = 0.78 and PSN_ND = 0.88) were found in this study (see Supplementary Information Table, Table 1 and Table 2).

The acquisition parameters of the 3D Multiple-GRE sequence for each scanner used in this study were shown in Supplementary Information Table, Table 5.

3.3. R_2^* And $R_{2(ISQR)}^*$ results

3.3.1. Parkinson's disease patients versus controls

All R_2^* values and $R_{2(ISQR)}^*$ values are displayed in Table 2. R_2^* values and $R_{2(ISQR)}^*$ values significantly increased in Parkinson's disease patients when compared with controls; in the substantia nigra in the dominant side and in the non-dominant side respectively (P_{SN_D} and $P_{SN\_ND} < 0.0001$; on both measures). In addition, R_2^* values significantly

increased in grey matter (grey matter = GM; $P_{GM} = 0.03$) and in white matter (white matter = WM; $P_{WM} = 0.03$).

3.3.2. Parkinson's disease patients according to disease duration

All the results of R_2^* values between the subgroups are summarized in Table 2. There was no significant difference for raw R_2^* values between the subgroups in all regions of interest.

$R_{2(ISQR)}^*$ values in the substantia nigra increased with the disease duration ($P_{SN\_D} = 0.01$; $P_{SN\_ND} = 0.03$). Fig. 2 presents the effect sizes between Parkinson's disease subgroups in the dominant side and non-dominant side in the substantia nigra using the $R_{2(ISQR)}^*$ values. The analyses were adjusted to HY, treatment, MDS-UPDRS part IV and quality of images. A significant difference in the effect size of $R_{2(ISQR)}^*$ values between Parkinson's disease subgroups ($P < 0.05$), as well as when comparing PD patients-G3. vs PD patients-G1 ($P_{SN\_D} = 0.03$, $P_{SN\_ND} = 0.01$) and when comparing PD patients-G4. vs PD patients-G1 ($P_{SN\_D} < 0.001$, $P_{SN\_ND} = 0.01$) was showed.

3.3.3. Parkinson's disease patients according to disease severity

During the course of the study, two new sub-groups were created based on the severity of the disease (H&Y < 2, $n = 28$ and H&Y ≥ 2, $n = 70$). Values are listed in Table 2. For all regions, no difference in R_2^*

Table 2

R_2^* values (s⁻¹) and $R_{2(ISQR)}^*$ values (s⁻¹) in each region of interest of PD group, PD subgroups and controls.

	All PD patients	Paired controls	Disease duration				Disease severity		P value
			PD patients G1	PD patients G2	PD patients G3	PD patients G4	PD patients (H&Y < 2)	PD patients (H&Y >= 2)	
R_2^*(raw data)									
Number of subjects	98	65	31	26	26	15	28	70	
SN_D	39.23 ± 5.85	34.94 ± 4.86	38.3 ± 4.53	39.48 ± 5.24	38.87 ± 7.71	41.96 ± 5.65	38.54 ± 4.89	39.51 ± 6.21	< 0.0001 [a]; 0.16[b]; 0.75[c]
SN_ND	38.88 ± 5.5	34.94 ± 4.86	37.29 ± 3.59	39.59 ± 5.63	39.63 ± 7.2	40.09 ± 5.18	38.28 ± 4.8	39.12 ± 5.77	< 0.0001 [a]; 0.37[b]; 0.8[c]
RN_D	33.42 ± 4.39	34.48 ± 4.83	33.35 ± 4	34.67 ± 4.82	32.75 ± 5.05	32.33 ± 2.46	34.75 ± 4.03	32.87 ± 4.44	0.14 [a]; 0.14[b]; 0.06[c]
RN_ND	33.51 ± 4.59	34.48 ± 4.83	33.84 ± 3.99	34.62 ± 5.31	32.35 ± 5.29	32.7 ± 1.92	34.13 ± 4.25	33.26 ± 4.72	0.19 [a]; 0.32[b]; 0.42[c]
GPi_D	28.64 ± 5.01	29.87 ± 4.72	29.57 ± 4.39	27.34 ± 4.15	28.67 ± 6.43	28.81 ± 4.99	28.39 ± 4.63	28.75 ± 5.19	0.1 [a]; 0.56[b]; 0.79[c]
GPi_ND	28.6 ± 4.4	29.86 ± 4.72	29.1 ± 4.36	28.06 ± 4.04	28.36 ± 4.93	28.89 ± 4.52	29.04 ± 4.57	28.43 ± 4.36	0.08 [a]; 0.74[b]; 0.49[c]
GPe_D	34.44 ± 4.22	35.3 ± 4.44	35.21 ± 3.44	34.32 ± 3.45	34.08 ± 5.51	33.33 ± 4.78	34.82 ± 3.98	34.29 ± 4.34	0.2 [a]; 0.75[b]; 0.73[c]
GPe_ND	34.76 ± 4.44	35.3 ± 4.44	34.89 ± 4.32	34.2 ± 3.33	35.25 ± 5.56	34.59 ± 4.63	35.18 ± 4.66	34.6 ± 4.37	0.44 [a]; 0.85[b]; 0.88[c]
STR_D	27.41 ± 3.21	28.46 ± 3.92	27.82 ± 2.92	27.54 ± 3.49	27.09 ± 3.63	26.7 ± 2.63	28.26 ± 2.98	27.07 ± 3.27	0.06 [a]; 0.81[b]; 0.13[c]
STR_ND	27.28 ± 3.06	28.46 ± 3.92	27.4 ± 3.08	27.49 ± 3.42	27.08 ± 2.75	26.96 ± 3.19	28.26 ± 3.07	26.88 ± 2.98	0.05 [a]; 0.92[b]; 0.06[c]
GM	20.1 ± 1.2	19.7 ± 1.3	–	–	–	–			**0.03** [a]
WM	20.8 ± 0.8	20.5 ± 0.8	–	–	–	–			**0.03** [a]
$R_{2(ISQR)}^*$)									
SN_D	6.05 ± 5.34	0.46 ± 1.92	4.83 ± 4.42	4.91 ± 4.47	6.48 ± 6.63	9.82 ± 4.5	3.98 ± 3.89	6.88 ± 5.64	< 0.0001 [a]; 0.01[b]; **0.02**[c]
SN_ND	5.36 ± 4.95	0.46 ± 1.92	3.44 ± 3.86	4.97 ± 4.53	7.28 ± 5.75	7.39 ± 5.03	4.14 ± 4.57	5.85 ± 5.05	< 0.0001 [a]; 0.03[b]; **0.09**[c]
GPi_D	−4.77 ± 5.84	−4.06 ± 5.52	−3.78 ± 5.12	−7.33 ± 6.48	−4.09 ± 6.4	−3.53 ± 3.69	−6.37 ± 5.93	−4.12 ± 5.72	0.47 [a]; 0.17[b]; 0.15[c]
GPi_ND	−4.91 ± 6.02	−4.06 ± 5.52	−4.76 ± 5.09	−6.56 ± 7.14	−3.98 ± 6.47	−3.81 ± 4.72	−5.1 ± 6.29	−4.83 ± 5.95	0.35 [a]; 0.72[b]; 0.8 [c]
GPe_D	1.02 ± 5.32	1.36 ± 4.6	1.86 ± 4.81	−0.35 ± 5.23	1.32 ± 6.52	1 ± 4.01	0.06 ± 5.64	1.41 ± 5.18	0.66 [a]; 0.38[b]; 0.19[c]
GPe_ND	1.25 ± 6.2	1.37 ± 4.61	1.04 ± 5.25	0.42 ± 6.67	2.89 ± 7.47	1.88 ± 4.12	1.04 ± 6.01	1.33 ± 6.32	0.89 [a]; 0.31[b]; 0.84[c]
STR_D	−6.01 ± 4.81	−5.48 ± 4.85	−5.52 ± 4.64	−7.13 ± 4.91	−5.67 ± 5.44	−5.63 ± 3.72	−6.5 ± 4.37	−5.8 ± 4.99	0.49 [a]; 0.69[b]; 0.42[c]
STR_ND	−6.23 ± 4.85	−5.48 ± 4.85	−6.44 ± 4.66	−7.13 ± 5.22	−5.28 ± 5.13	−5.74 ± 4.11	−5.87 ± 4.22	−6.37 ± 5.1	0.72 [a]; 0.8 [b]; 0.73[c]

Values are expressed as Mean ± standard deviation; PD = Parkinson's disease; na = not applicable; SN_D = substantia nigra_dominant; SN_ND = substantia nigra_non dominant; RN_D = red nucleus_dominant; RN_ND = red nucleus_non dominant; GPe = globus pallidus externus_dominant; GPe = globus pallidus externus_non dominant; GPi_D = globus pallidus internus_dominant; GPi_ND = globus pallidus internus_non dominant; STR_D = striatum_dominant; STR_ND = striatum_non dominant; GM = grey matter; WM = white matter. G1: Group1 < 5 years; G2: Group2 > 5 and ≤ 10 years; G3: Group3 > 10 and ≤ 15 years, G4: Group4 > 15 years.

[a] : statistical significance between PD patients and healthy controls.

[b] : statistical significance between the PD subgroups according to disease duration.

[c] : statistical significance between the PD subgroups according to disease severity.

values was found between these two subgroups. However, there was a significant increase in $R_{2(ISQR)}^*$ values in patients with H&Y ≥ 2 compared to H&Y < 2 in the substantia nigra in the dominant side of the disease (P_{SN_D} = 0.02).

3.3.4. Correlation results of R_2^* / $R_{2(ISQR)}^*$

Positive correlations of regional R_2^* rate constants in the substantia nigra for MDS-UPDRS-IV (r_{SN_D} = 0.33, P_{SN_D} = 0.002 and r_{SN_ND} = 0.35, P_{SN_ND} = 0.001) and for LEDD (r_{SN_D} = 0.25, P_{SN_D} = 0.02 and r_{SN_ND} = 0.27, P_{SN_ND} = 0.01) and negatives correlations between R_2^* values and MDS-UPDRS-I in -GPe (r_{GPe_D} = -0.27, P_{GPe_D} = 0.01; r_{GPe_ND} = -0.33, P_{GPe_ND} = 0.002), and in -GPi (r_{GPi_D} = -0.29, P_{GPi_D} = 0.01; r_{GPi_ND} = -0.38, P_{GPi_ND} = 0.002) and negatives correlations between R_2^* values and MDS-UPDRS-III in -STR (r_{STR_D} = -0.23, P_{STR_D} = 0.03; r_{STR_ND} = -0.27, P_{STR_ND}

= 0.01) and negatives correlations between R_2^* values and ASBPD_I&II in -GPe (r_{GPe_ND} = -0.21, P_{GPe_ND} = 0.05) and in -GPi (r_{GPi_D} = -0.23, P_{GPi_D} = 0.04; r_{GPi_ND} = -0.31, P_{GPi_ND} = 0.003) were found (Fig. 3A).

Positive correlations were found between the $R_{2(ISQR)}^*$ in the substantia nigra and clinical features: disease duration (r_{SN_D} = 0.23, $_{SN\_D}$ = 0.03, and r_{SN_ND} = 0.28, P_{SN_ND} = 0.01), H&Y stages (r_{SN_D} = 0.24, P_{SN_D} = 0.02), MDS-UPDRS-IV (r_{SN_D} = 0.24, P_{SN_D} = 0.02, and r_{SN_D} = 0.32, P_{SN_ND} = 0.003) and with LEDD (r_{SN_D} = 0.21, P_{SN_D} = 0.04, and r_{SN_ND} = 0.3, P_{SN_ND} = 0.01). In addition, a positive correlation was found between the $R_{2(ISQR)}^*$ and age in substantia nigra (r_{SN_D} = 0.29, P_{SN_D} = 0.004). Finally, negative correlations were found between $R_{2(ISQR)}^*$ values in -GPe and -GPi, and MDS-UPDRS-I (r_{GPe_D} = -0.29, P_{GPe_D} = 0.01; r_{GPe_ND} = -0.28, P_{GPe_ND} = 0.01) (r_{GPi_D} = -0.27, P_{GPi_D} = 0.01, r_{GPi_ND} = -0.34, P_{GPi_ND} = 0.001), and in -GPe and MDS-UPDRS-II (r_{GPe_D} =
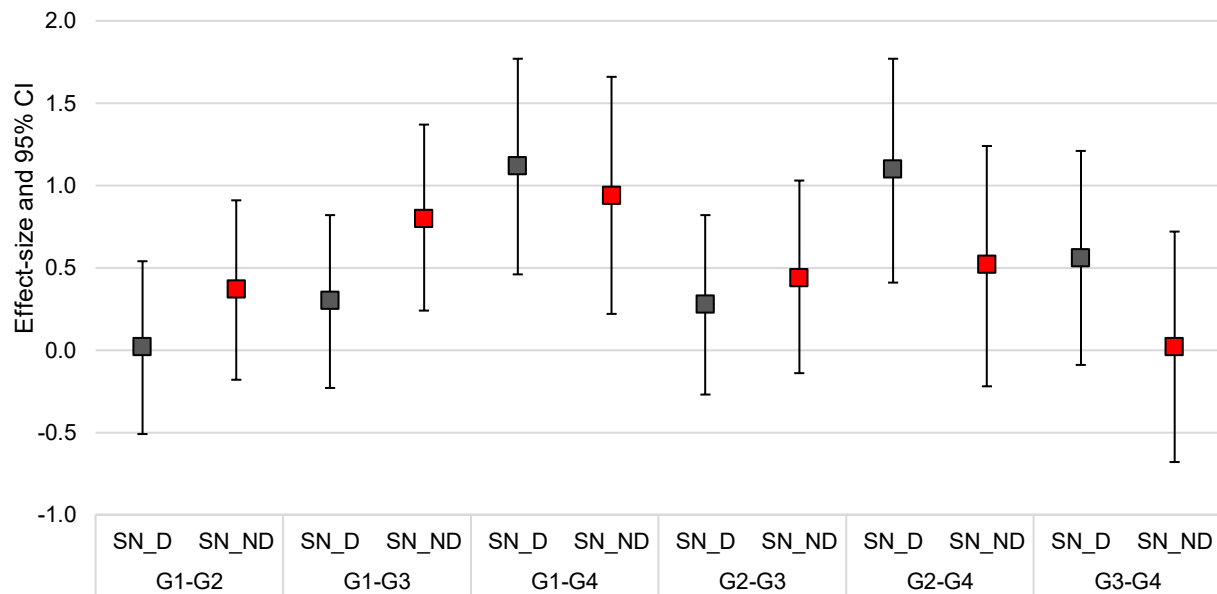
Fig. 2. Forest plot showing the crude effect size of $R^*_{2(ISQR)}$ in the substantia nigra for each Parkinson's disease (PD) subgroup according to the disease duration: G1 (PD < 5 years), G2 (PD > 5 and < 10 years), G3 (PD > 10 and < 15 years) and G4 (PD > 15 years). G1-G2: effect size between G1 and G2, G1-G3: effect size between G1 and G3, G1-G4: effect size between G1 and G4, G2-G3: effect size between G2 and G3, G2-G4 effect size between G2 and G4, G3-G4: effect size between G3 and G4. SN_D = substantia nigra_dominant side of the diease. SN_ND = substantia nigra_ non dominant side of the disease. The results were expressed using Hedge's effect size. CI = confidence interval. The box represents the effect size and the whiskers the 95 % CI. A significant difference in the effect size of $R^*_{2(ISQR)}$ values between Parkinson's disease subgroups ($P < 0.05$), as well as when comparing PD patients-G3. vs PD patients-G1 ($P_{SN\_D} = 0.03$, $P_{SN\_ND} = 0.01$) and when comparing PD patients-G4. vs PD patients-G1 ($P_{SN\_D} < 0.001$, $P_{SN\_ND} = 0.01$) was showed.

-0.3, $P_{GPe\_D} = 0.005$ and $r_{GPe\_ND} = -0.23$, $P_{GPe\_ND} = 0.04$) in the -GPe, in -GPi and MDS-UPDRS IV ($r_{GPe\_D} = -0.32$, $P_{GPe\_D} = 0.003$ and $r_{GPi\_D} = -0.3$, $P_{GPi\_D} = 0.005$ and $r_{GPi\_ND} = -0.27$, $P_{GPi\_ND} = 0.01$) (Fig. 3B).

3.3.5. Discriminant factorial analysis

In Fig. 4A, the results show the relationship between the $R^*_{2(ISQR)}$ values of the patients and the clinical parameters included in this study. As described previously, a moderate correlation between $R^*_{2(ISQR)}$ substantia nigra values and clinical data was highlighted. In Fig. 4B, clusters related to disease duration were satisfactorily separated. In this discriminant factorial analysis, the two first components represented 77 % of variability. The first one (noted CompA1) was mainly related to severity of disease and the second (noted CompA2) to $R^*_{2(ISQR)}$ substantia nigra values in the dominant side of the disease. When only $R^*_{2(ISQR)}$ values of patients in all regions of interest (without clinical data) were retained to conduct factorial analysis, patients were better discriminated according to disease duration (Fig. 4C), principally due to $R^*_{2(ISQR)}$ values in the substantia nigra in the dominant side (noted CompB2) whereas CompB1 expressed the magnitude of $R^*_{2(ISQR)}$ values in the dominant side, whatever the region (Fig. 4D). For this second discriminant factorial analysis, 89 % of variability was assessed.

4. Discussion

In this multicentre study, the changes in R^*_2 relaxation rate, which reflects iron concentration, was studied as a function of the duration and severity of Parkinson's disease, while taking into account the inter-subject variability of the R^*_2 parameter. We first considered the average R^*_2 within several basal ganglia regions and then developed an original approach using an internal reference in order to highlight the variation in R^*_2 linked to Parkinson's disease compared to other sources of R^*_2 variance.

Our ISQR approach allowed us to obtain a significant difference

when comparing the different groups of patients to their controls. When analyses were controlled by H&Y, treatment, MDS-UPDRS part IV and quality as covariables in multivariate analyses in addition to centre and machine as random-effects, the results were not changed. In addition, ISQR can be used to show a progressive increase of the magnitude effect of the $R^*_{2(ISQR)}$ parameter in the substantia nigra in parkinsonian patients according to the disease duration, taking into account the paired effect, the centre and machine effects and image quality. Finally, correlations are also observed between the $R^*_{2(ISQR)}$ of several regions of interest with the clinical characteristics of Parkinson's disease (age, duration of disease, severity, motor and non-motor symptoms). This is in line with current concepts recognizing that dysfunctions within the basal ganglia induce cognitive and behavioral deficits in addition to the motor symptoms of Parkinson's disease (Tremblay et al., 2015). These results enable to consider the use of this parameter as a potential marker of the progression of the disease.

4.1. Comparison of the results with previous studies

In our study, a significant difference was shown for R^*_2 values between patients with Parkinson's disease and control subjects in the substantia nigra, which was consistent with the results of most previous studies (Graham et al., 2000; Martin and Gee, 2008; Péran et al., 2010; Du et al., 2012; Ulla et al., 2013; Wieler et al., 2015; Pyatigorskaya et al., 2015) except those by (Reimão et al., 2015).

In addition and especially without applying the ISQR approach, no effect of disease duration and severity assessed with H&Y scale on R^*_2 parameters were shown in our study. These results are in line with previous R^*_2 – based cross-sectional studies (Gorell et al., 1995; Graham et al., 2000; Martin and Gee, 2008; Péran et al., 2010; Du et al., 2011; Barbosa et al., 2015; Cheng et al., 2020) which also did not find a significant correlation between the regional iron levels and disease duration. However, He et al. (He et al., 2015) reported a positive correlation between increased susceptibility values in the substantia nigra and disease duration in patients with Parkinson's disease, but the elevated
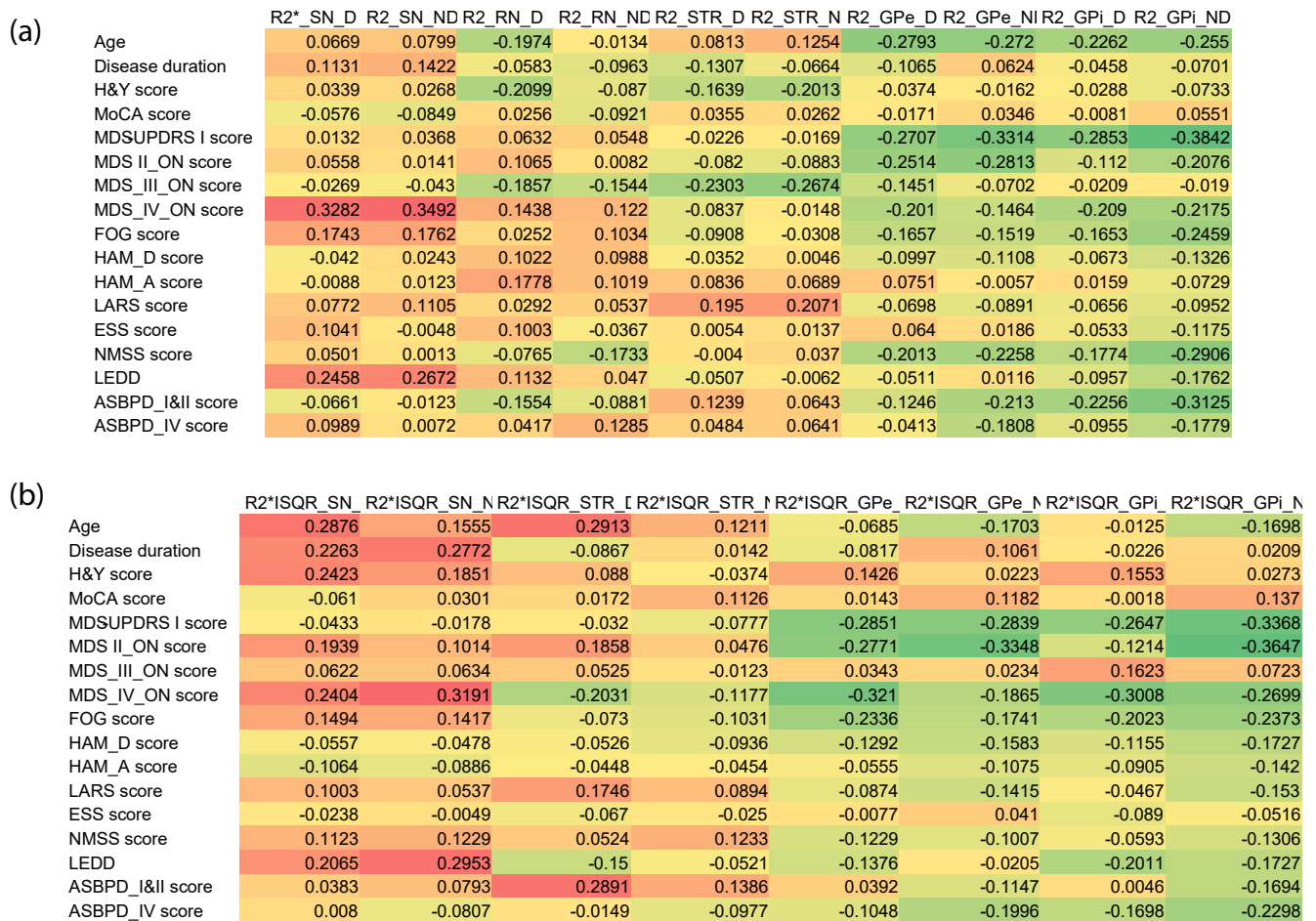
(a)

	R2*_SN_D	R2_SN_ND	R2_RN_D	R2_RN_ND	R2_STR_D	R2_STR_N	R2_GPe_D	R2_GPe_Nl	R2_GPi_D	R2_GPi_ND
Age	0.0669	0.0799	-0.1974	-0.0134	0.0813	0.1254	-0.2793	-0.272	-0.2262	-0.255
Disease duration	0.1131	0.1422	-0.0583	-0.0963	-0.1307	-0.0664	-0.1065	0.0624	-0.0458	-0.0701
H&Y score	0.0339	0.0268	-0.2099	-0.087	-0.1639	-0.2013	-0.0374	-0.0162	-0.0288	-0.0733
MoCA score	-0.0576	-0.0849	0.0256	-0.0921	0.0355	0.0262	-0.0171	0.0346	-0.0081	0.0551
MDSUPDRS I score	0.0132	0.0368	0.0632	0.0548	-0.0226	-0.0169	-0.2707	-0.3314	-0.2853	-0.3842
MDS II_ON score	0.0558	0.0141	0.1065	0.0082	-0.082	-0.0883	-0.2514	-0.2813	-0.112	-0.2076
MDS_III_ON score	-0.0269	-0.043	-0.1857	-0.1544	-0.2303	-0.2674	-0.1451	-0.0702	-0.0209	-0.019
MDS_IV_ON score	0.3282	0.3492	0.1438	0.122	-0.0837	-0.0148	-0.201	-0.1464	-0.209	-0.2175
FOG score	0.1743	0.1762	0.0252	0.1034	-0.0908	-0.0308	-0.1657	-0.1519	-0.1653	-0.2459
HAM_D score	-0.042	0.0243	0.1022	0.0988	-0.0352	0.0046	-0.0997	-0.1108	-0.0673	-0.1326
HAM_A score	-0.0088	0.0123	0.1778	0.1019	0.0836	0.0689	0.0751	-0.0057	0.0159	-0.0729
LARS score	0.0772	0.1105	0.0292	0.0537	0.195	0.2071	-0.0698	-0.0891	-0.0656	-0.0952
ESS score	0.1041	-0.0048	0.1003	-0.0367	0.0054	0.0137	0.064	0.0186	-0.0533	-0.1175
NMSS score	0.0501	0.0013	-0.0765	-0.1733	-0.004	0.037	-0.2013	-0.2258	-0.1774	-0.2906
LEDD	0.2458	0.2672	0.1132	0.047	-0.0507	-0.0062	-0.0511	0.0116	-0.0957	-0.1762
ASBPD_I&II score	-0.0661	-0.0123	-0.1554	-0.0881	0.1239	0.0643	-0.1246	-0.213	-0.2256	-0.3125
ASBPD_IV score	0.0989	0.0072	0.0417	0.1285	0.0484	0.0641	-0.0413	-0.1808	-0.0955	-0.1779

(b)

	R2*ISQR_SN_	R2*ISQR_SN_N	R2*ISQR_STR_[	R2*ISQR_STR_N	R2*ISQR_GPe_	R2*ISQR_GPe_N	R2*ISQR_GPi_	R2*ISQR_GPi_N
Age	0.2876	0.1555	0.2913	0.1211	-0.0685	-0.1703	-0.0125	-0.1698
Disease duration	0.2263	0.2772	-0.0867	0.0142	-0.0817	0.1061	-0.0226	0.0209
H&Y score	0.2423	0.1851	0.088	-0.0374	0.1426	0.0223	0.1553	0.0273
MoCA score	-0.061	0.0301	0.0172	0.1126	0.0143	0.1182	-0.0018	0.137
MDSUPDRS I score	-0.0433	-0.0178	-0.032	-0.0777	-0.2851	-0.2839	-0.2647	-0.3368
MDS II_ON score	0.1939	0.1014	0.1858	0.0476	-0.2771	-0.3348	-0.1214	-0.3647
MDS_III_ON score	0.0622	0.0634	0.0525	-0.0123	0.0343	0.0234	0.1623	0.0723
MDS_IV_ON score	0.2404	0.3191	-0.2031	-0.1177	-0.321	-0.1865	-0.3008	-0.2699
FOG score	0.1494	0.1417	-0.073	-0.1031	-0.2336	-0.1741	-0.2023	-0.2373
HAM_D score	-0.0557	-0.0478	-0.0526	-0.0936	-0.1292	-0.1583	-0.1155	-0.1727
HAM_A score	-0.1064	-0.0886	-0.0448	-0.0454	-0.0555	-0.1075	-0.0905	-0.142
LARS score	0.1003	0.0537	0.1746	0.0894	-0.0874	-0.1415	-0.0467	-0.153
ESS score	-0.0238	-0.0049	-0.067	-0.025	-0.0077	0.041	-0.089	-0.0516
NMSS score	0.1123	0.1229	0.0524	0.1233	-0.1229	-0.1007	-0.0593	-0.1306
LEDD	0.2065	0.2953	-0.15	-0.0521	-0.1376	-0.0205	-0.2011	-0.1727
ASBPD_I&II score	0.0383	0.0793	0.2891	0.1386	0.0392	-0.1147	0.0046	-0.1694
ASBPD_IV score	0.008	-0.0807	-0.0149	-0.0977	-0.1048	-0.1996	-0.1698	-0.2298

Fig. 3. Heatmap of correlations between clinical features, R_2^* values and $R_{2(ISQR)}^*$ values. The heatmap colors range is **red** when a significant positive correlation ($P < 0.01$), is **orange** when a significant positive correlation ($P < 0.05$), is **dark green** when a significant negative correlation ($P < 0.01$), is **light green** when a significant negative correlation ($P < 0.05$) and it is **yellow** when there is not significant: (A) R_2^* raw values. (B) $R_{2(ISQR)}^*$ values. SN_D = substantia nigra_dominant; SN_ND = substantia nigra_non dominant; RN_D = red nucleus_dominant; RN_ND = red nucleus_non dominant; GPe = globus pallidus externus_dominant; GPe = globus pallidus externus_non dominant; GPi_D = globus pallidus internus_dominant; GPi_ND = globus pallidus internus_non dominant; STR_D = striatum_dominant; STR_ND = striatum_non dominant. MoCA = Montreal Cognitive Assessment, MDS-UPDRS = Movement Disorder Society-Unified Parkinson's Disease Rating Scale, H&Y = Hoehn & Yahr score, S&E = Schwab & England score, FOG-Q = Freezing of Gait Questionnaire, LARS = Lille Apathy Rating Scale, HAM-D = Hamilton Rating Scale for Depression, HAM-A = Hamilton Rating Scale for Anxiety, ASBPD = Ardouin Scale of Behavior in Parkinson's Disease, NMSS = Non-Motor Symptom assessment Scale for Parkinson's Disease, LEDD = Levodopa Equivalent Daily Dose. (For interpretation of the references to color in this figure legend, the reader is referred to the web version of this article.)

R_2^* values in the substantia nigra were not correlated with clinical features. Langkammer et al. (Langkammer et al., 2016) demonstrated that the substantia nigra susceptibility values were correlated with H&Y scales but were not correlated with disease duration in patients with Parkinson's disease. Finally, if longitudinal studies have confirmed that variation in R_2^* may capture Parkinson's disease-related progression in the substantia nigra (Du et al., 2018; Hopes et al., 2016; Ulla et al., 2013), others failed to detect a longitudinal change (Arribarat et al., 2019; Wieler et al., 2015).

The previous attempts at finding correlations between R_2^* and severity or disease duration are somewhat contradictory. This may be explained by different sources of variability that reduce the sensitivity and accuracy of R_2^* mapping. Variability can be due to the heterogeneity of the studied populations and also to instrumental variability (i.e. noise). Moreover, part of the inter-subject variability may be unrelated to disease. This is the main reason that led to develop the ISQR strategy with the aim of reducing large inter-subject variability (10–20 %) not related to disease in the regions of interest.

4.2. ISQR strategy interest

ISQR is introduced for the first time in this study. It is based on the finding that a significant part of the inter-subject variability of R_2^* in most subcortical regions is not related to Parkinson's disease. By removing most of this variability using ISQR, our results allowed us to estimate the effect size due to Parkinson's disease as function of the duration and severity of the disease. It shows that this effect size is comparable to the unexplained variance. For example, when comparing patients of Group 1 with controls, the difference of R_2^* values in the substantia nigra obtained by ISQR was 3 and 4.4 s^{-1} on the dominant side and in the non dominant side of the disease respectively, which corresponded to the level of the inter-subject variance of controls under our experimental conditions (e.g. 5.5 s^{-1}, the standard deviation of R_2^* in the substantia nigra of controls). This explains why, without the ISQR approach, we failed to demonstrate any significant differences between subgroups of patients with Parkinson's disease.

ISQR was developed using R_2^* in the red nucleus as an intra-subject reference. It deserves to come back in more detail to the reasons for choosing this reference and especially on two results obtained from the
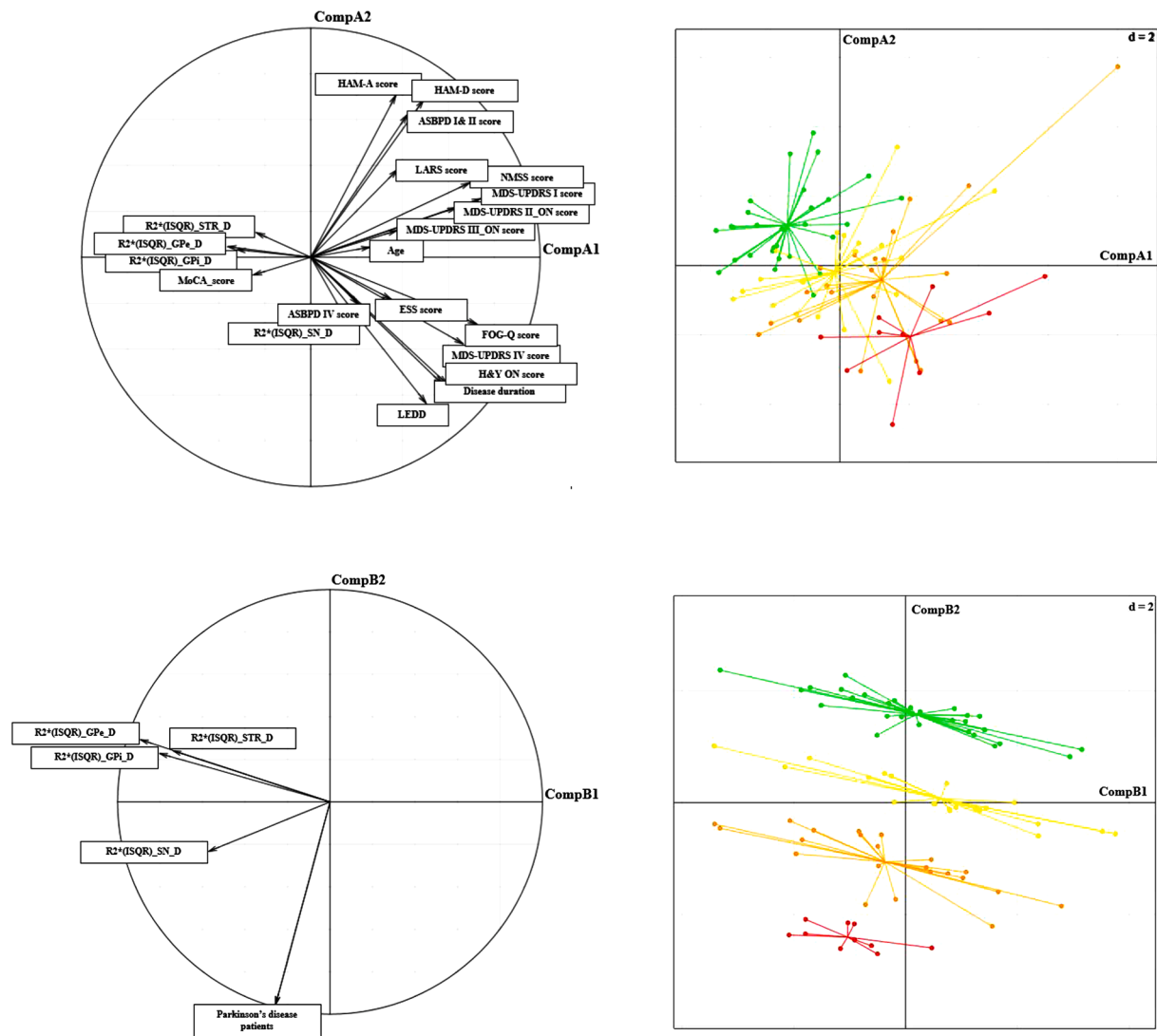
Fig. 4. Two-dimensional plot based on principal component analysis. (A) Plot represents the relationships between the $R^*_{2(ISQR)}$ values of Parkinson's disease patients and the clinical parameters included in this study. (B) Four distinct profiles of Parkinson's disease patients according to the disease duration, illustrated by factorial analysis. The length of the arrows indicates the magnitude of the relationship to the $R2^*_{ISQR}$ and clinical parameters, the first one (noted **CompA1**) was most related to severity of disease and the second (noted **CompA2**) to $R^*_{2(ISQR)}$ substantia nigra values. Each dot represents one Parkinson's disease patient. (C) Plot represents the relationships between the $R^*_{2(ISQR)}$ values in the dominant side of Parkinson's disease patients for each region of interest (D) Four distinct profiles of Parkinson's disease patients according to the disease duration, illustrated by factorial analysis. The length of the arrows indicates the magnitude of the relationship to the $R2^*_{ISQR}$ **without clinical parameters**. Parkinson's disease patients were correctly discriminated according to their disease duration, principally due to $R^*_{2(ISQR)}$ values in substantia nigra (noted **CompB2**) whereas **CompB1** expressed the magnitude of $R^*_{2(ISQR)}$ values whatever the region. Each dot represents one Parkinson's disease patient. Parkinson's disease = PD. The **red** color corresponds to PD patients > 15 years, the **orange** to PD patients > 10 and < 15 years, the **yellow** to PD patients > 5 and < 10 years and the **green** to PD patients < 5 years. (For interpretation of the references to color in this figure legend, the reader is referred to the web version of this article.)

control subjects. First, the inter-subject R^*_2 variability in the red nucleus was equivalent to the one measured in the other regions of interest. Secondly, we found that R^*_2 in the red nucleus and in the substantia nigra were highly correlated. Additionally, studies similar to ours did not find a difference in R^*_2 between parkinsonian patients and control subjects in the red nucleus (Barbosa et al., 2015; Martin and Gee, 2008; Murakami et al., 2015; Langkammer et al., 2016; Cheng et al., 2020) except in the work of Lewis (Lewis et al., 2013) who found an increase in the value of R^*_2 in parkinsonian patients with dyskinesia when compared to controls but no difference in Parkinson's disease patients without dyskinesia when compared to controls. Unfortunately, no postmortem study is currently available to accurately assess the iron amount in red nuclei of patients with Parkinson's disease. Due to the current lack of

understanding, we cannot definitively say whether or not the red nuclei play a role in Parkinson's disease. But our in vivo results bring several convincing results suggesting that choosing these nuclei as a reference is efficient to remove the R^*_2 variations unrelated to the disease.

As mentioned in the introduction, R^*_2 is not considered to be very sensitive biomarker, especially compared to the recent method based on the acquisition of T1-weighted neuromelanin (NM)-sensitive imaging. The study by Gaurav (Gaurav et al., 2021) showed variations of measured SN volume induced by Parkinson's disease. The data published permitestimating the effect size at 0.76 in a diseased group (duration of progression <4 years) compared to a control group. In our R2* study, the effect size for group 1 (duration of progression <5 years) is 0.71/0.53 for dominant and non-dominant sides respectively, thus

slightly less, pointing to lower sensitivity for the raw R2* approach compared to NM. However, using ISQR boosted the effect size which reached 1.50/1.12 for this group. This shows that ISQR is a pertinent means of increasing the sensitivity of the method based on R2* to the point of exceeding that of the T1-NM approach. Moreover, this increase in sensitivity linked to ISQR was confirmed for all the other groups (see Supplementary Information Table, Table 4).

4.3. Origin of R_2* signal and variability

An interesting point to note is that for controls, neither the inter-subject R_2^* variations in the cortex nor those in the white matter are correlated with variations in subcortical regions (Supplementary Table 3). This is why these extended regions cannot serve as internal references for ISQR in the same way as the red nuclei do. In addition, since the inter-subject R_2^* variations in the subcortical regions are greater than in the rest of the brain and are strongly correlated, these variations probably originate from biological factors which specifically modify the R_2^* relaxation in these regions. Indeed, it is very unlikely that instrumental variations could explain such an inter-subject correlation of R_2^* specifically in subcortical regions.

It is therefore necessary to question the biological factors which are able to shift the R_2^* in the subcortical structures from one subject to another. Iron is undoubtedly the most important determinant of R_2^* relaxation in the human brain. To such an extent that initially, R_2^* mapping was suggested as an indicator of iron content (Gelman et al., 1999). Since iron is distributed in different forms at the cellular level, the relationship between iron concentration and R_2^* is not yet well established. The two major forms of iron are neuromelanin within the dopaminergic neurons and ferritin stored outside the dopaminergic neurons. Importantly, no particular hyperintensity was exhibited in the red nucleus using neuromelanin-weighted MRI (Trujillo et al., 2017). It can therefore be hypothesized that the R_2^* in the red nucleus and probably also in basal ganglia (i.e. striatum, globus pallidus) is mainly influenced by ferritin concentration. In sum, ferritin could be the biological factor which induces the inter-subject variations unrelated to Parkinson's disease. Our results support this hypothesis and justify the use of the ISQR approach by taking the red nucleus as a reference to reflect the ferritin amount within the basal ganglia of each subject and thus emphasizing the variations due to neuromelanin.

Previous studies have shown that R_2^* does not only reflect the iron content. Experimental factors such as the orientation of the head in the scanner and small deviations of magnetic field strength can induce R_2^* variations (Azuma et al., 2016; Yablonskiy and Haacke, 1994; Li et al., 2012). Besides, due to the non-local nature of the magnetic field, R_2^* relaxation is prone to blooming artifacts, i.e. it depends both on local iron in a voxel and on the presence of other structures outside the voxel of interest which generate magnetic field variations due to susceptibility differences (Stüber and Wang, 2016). Due to the latter mechanism, R_2^* variations may partly be due to inter-subject differences of myelination (Duyn, 2017). This effect is unlikely to be significant here due to the absence of correlation between R_2^* in white matter and in subcortical regions.

4.4. Limitations-strengths

Many subjects were excluded from the current analysis after image quality control. As the number of patients with later stage Parkinson's disease was limited, a contrast analysis between early-stage Parkinson's disease subjects and later-stage Parkinson's disease subjects was not performed. Moreover the MRI sequence was a fast multiple GRE which was prone to motion artifact and thus may explain the higher exclusion rate for patients, especially for later stages of disease evolution (see Fig. 1).

Obtaining quality acquisitions is a challenge since the propensity to perform abnormal movements during an exam (e.g., tremor, dyskinesia) is characteristic of Parkinsonian patients. Constant progress has been achieved in reducing the duration of sequences (e.g., 6min10s, Barbosa, J. H et al., 2015) since this acceleration reduces the possibility that a parasite movement of the patient occurs during acquisition. However, an intrinsic characteristic of high-speed sequences is the reduction of dead time, thus making more likely that a parasite movement occurs during an impactful period. Recent real time strategies based on suspending data acquisition during these periods are relevant (Castella et al., 2018) and could significantly improve the quality of R2* of future studies while reducing the level of rejection.

In our study, the red nucleus was chosen as a reference region for normalization because of its proximity to the substantia nigra, R2* values close to those of the substantia nigra, a lack of significant differences in R2* between patients and controls in this region in our study and in the majority of recent studies (Barbosa et al., 2015; Martin and Gee, 2008; Murakami et al., 2015; Langkammer et al., 2016; Cheng et al., 2020), except for differences reported by Lewis et al in patients with dyskinesia but not in patients without dyskinesia. However, when iron content in RN was assessed by quantitative susceptibility mapping (QSM), the reported results were contrasted with an increase in QSM signal (Sethi et al, 2019, Langkammer et al, 2016) or no significant variation (He et al, 2015, Azuma et al, 2016, Du et al, 2018). Furthermore, several studies have shown an increase in the volume of the RN in Parkinsonian patients (Colpan and Slavin, 2010; Camladig et al 2014, Shah et al, 2020; Kolpakwar et al 2021) interpreted as a compensatory phenomenon linked to Parkinson's disease, as the RN has many indirect and direct connections to motor coordinating pathways. Finally, and unfortunately, no *post mortem* data on RN in Parkinson's disease is available, which limits our understanding of the role of this nucleus in the pathophysiology of Parkinson's disease. Even if the involvement of RN in Parkinson's disease is poorly understood, the magnitude of the disease's effect on R2*, if present, is small in this structure compared to that observed in SN. This is why this region can be chosen to serve as an internal reference.

In this paper, we present the results of our subjects at baseline. Our on-going longitudinal follow-up will be essential in confirming the dynamic changes of R_2^* during disease progression by applying the ISQR approach.

Performing MRI acquisitions in different centres and with various machines introduces further variability. In our study, MRI machines and sequences were normalized to reduce this instrumental variability. No differences were found between centres and machines. This validates the precautions taken for normalizing the acquisition protocol. However, many other instrumental factors impact data quality during the acquisition stage (choice of TEs, coils and sequences). Post-processing (motion correction, normalization, spatial filtering, region segmentation) (Fernández-Seara, 2000; Kennan and Gore, 1994) affects data quality as well. If the proposed quantitative approach is based on proven open-access tools, it is very likely that the intra-subject variability can be further reduced by using up-to-date post-processing tools.

As clusters of substantia nigra pars compacta neurons are deeply embedded within the substantia nigra pars reticulata, the boundary between these two structures in humans is difficult to define, in particular in its caudal part (Prensa and Parent, 2001). Moreover, spatial correspondence between histology and MRI of the substantia nigra at 1.5 and 3T is not precise (Lehéricy et al., 2014). For this reason, we decided to refer to the substantia nigra as a whole for data analysis.

Considering that iron at the cellular level is distributed in different forms, this can presumably lead to distinct decaying behaviors as a function of TE, monoexponential for neuromelanin and quadratic exponential for ferritin (Brammerloh et al., 2018). Due to our limited range of echo times, these two lineshapes could not be disentangled. Thus, both contribute to the R_2^* obtained from the monoexponential fit.

A prerequisite when attempting to separate these two compartments would be to acquire low noise echo trains in a wider time range. This remains a challenge in clinical imaging conditions.

Quantitative susceptibility mapping may be an alternative approach which appears to be more sensitive than using R_2^* (Cheng et al., 2020). However, the susceptibility mapped by any technique is likely to be influenced by interindividual variability unrelated to the disease. Hence ISQR could improve this approach as well.

5. Conclusion

Our results indicate that R_2^* mapping is a technique that can detect subtle iron-related variations in subcortical regions of Parkinson's disease patients. However, certain conditions are necessary to eliminate variations not directly related to the disease. Both inter-subject variability and intra-subject variability, could explain the earlier, sometimes contradictory results obtained by quantitative MRI-R_2^*. Our ISQR strategy greatly improves the specificity of MRI-R_2^* and designates R_2^* a possible biomarker for monitoring the evolution of Parkinson's disease.

Declaration of Competing Interest

The authors declare that they have no known competing financial interests or personal relationships that could have appeared to influence the work reported in this paper.

Data availability

No data was used for the research described in the article.

Appendix A

R_2^* study group

Investigators:
Debilly Bérengère, Derost Philippe, Ulla Miguel; Clermont-Ferrand University Hospital, Department of Neurology and NS-Park/FCRIN Network, 63,000 Clermont-Ferrand, France.

Devos David, Grolez Guillaume; Inserm, Department of Movement Disorder and NS-Park/FCRIN Network, 1172 University of Lille, France.

Castrioto Anna, Meoni Sara; Movement Disorders Unit, University Hospital Center, Grenoble Alpes University, Grenoble Institute of Neuroscience, UGA INSERM U1216 and NS-Park/FCRIN Network, Grenoble, France.

Plus Bruno; Hospices Civils of Lyon, Neurological Hospital Pierre Wertheimer, Department of Neurology, Lyon, France.

Boraud Thomas, Laurens Brice; Department of Neurology, CHU Bordeaux, 33,000 Bordeaux, France.

Hopes Lucie; Department of Neurology, CHRU Nancy.

Ansquer Solène, Benatru Isabelle; INSERM CIC-1402, Department of Neurology, CHU of Poitiers, University of Poitiers.

Calvas Fabienne, Galitzky Monique, Senard Ana, Thalamas Claire; Centre d'Investigation Clinique CIC 1436, UMR 1214 TONIC and NS-Park/FCRIN Network; INSERM, CHU of Toulouse, University of Toulouse3, Toulouse, France.

Neuropsychologists:

Delaby Laure, Vidal Tiphaine; Clermont-Ferrand University Hospital, Department of Neurology, 63,000 Clermont-Ferrand, France.

Delliaux Marie, Dujardin Kathy, Brion Marine; Inserm, Department of Movement Disorder, 1172 University of Lille, France.

Lhommee Eugénie, Bichon Amelie, Baudet Laurène; Grenoble University Hospital, Department of Neurology, University Grenoble Alpes, Grenoble Institute of Neuroscience, Grenoble, France.

Klinger Hélène; Hospices Civils of Lyon, Neurological Hospital Pierre Wertheimer, Department of Neurology, Lyon, France.

Benchetrit Marie, Pineau Fanny, Socha Julie; Sorbonne University, Inserm, CNRS, Paris Brain Institute—ICM, Assistance Publique Hôpitaux de Paris, Hôpital Pitié-Salpêtrière, Department of Neurology, Clinical Investigation Center for Neurosciences, NS-PARK/FCRIN Network, Paris, France.

Auzou Nicolas, Bonnet Marie; Department of Neurology - Maladies Neurodégénératives, CHU Bordeaux, F-33000 Bordeaux, France.

Dillier Céline, Meyer Mylène; Department of Neurology, CHRU Nancy.

Saenz Amaya; Department of Neurology, Hôpital Maison blanche, Reims, France.

Lemoine Laurine; Centre Expert Parkinson, CHU Henri Mondor, AP-HP et Equipe Neuropsychologie Interventionnelle, INSERM-IMRB, Faculté de Santé, Université Paris-Est Créteil et Ecole Normale Supérieure Paris Sorbonne Université.

Fradet Anne, Manssouri Anziza; INSERM CIC-1402, Department of Neurology, CHU of Poitiers, University of Poitiers.

Bayet Virginie, Nuz Sophie, Pierre Michèle, Pomies Elsa; Centre d'Investigation Clinique CIC 1436, UMR 1214 TONIC and NS-Park/FCRIN Network; INSERM, CHU of Toulouse, University of Toulouse3, Toulouse, France.

Neuroradiologists:

Jean Betty; Clermont-Ferrand University Hospital, Department of Neurology, F-63000 Clermont-Ferrand, France.

Delmaire Christine, Dumont Julien; Inserm, Department of Movement Disorder, 1172 University of Lille, France.

Krainik Alexandre, Tropes Irène; Grenoble University Hospital, Department of Neurology, University Grenoble Alpes, Grenoble Institute of Neuroscience, Grenoble, France.

Ibarrola Danielle; Hospices Civils of Lyon, Neurological Hospital Pierre Wertheimer, Department of Neurology, Lyon, France.

Didier Mélanie, Humbert Frédéric; Sorbonne University, Paris Brain Institute—ICM, Assistance Publique Hôpitaux de Paris, Paris, France.

Le Bars Emmanuelle; Department of Neuroradiology, Montpellier University Hospital Center, Gui de Chauliac Hospital, Montpellier, France.

Buisson Caroline, Sibon Igor; Department of Neurology - Maladies Neurodégénératives, CHU Bordeaux, F-33000 Bordeaux, France.

Portefaix Christophe; Department of Neurology, Hôpital Maison blanche, Reims, France.

Lincot Julien; Centre Expert Parkinson, CHU Henri Mondor, AP-HP et Equipe Neuropsychologie Interventionnelle, INSERM-IMRB, Faculté de Santé, Université Paris-Est Créteil et Ecole Normale Supérieure Paris Sorbonne Université.

Guillevin Remy; INSERM CIC-1402, Department of Neurology, CHU of Poitiers, University of Poitiers.

Gros Hélène; Centre d'Investigation Clinique CIC 1436, UMR 1214 TONIC and NS-Park/FCRIN Network; INSERM, CHU of Toulouse, University of Toulouse3, Toulouse, France.

Clinical research Engineers:

Bernard Stéphane, Rieu Isabelle; Clermont-Ferrand University Hospital, Department of Neurology, F-63000 Clermont-Ferrand, France.

Pleuvret Marie; Inserm, Department of Movement Disorder, 1172 University of Lille, France.

Pelissier Pierre; Grenoble University Hospital, Department of Neurology, University Grenoble Alpes, Grenoble Institute of Neuroscience, Grenoble, France.

Brochard Vanessa, Le Toullec Benjamin; Sorbonne University, Paris Brain Institute—ICM, Assistance Publique Hôpitaux de Paris, Paris, France.

David Gay, Sonia Djobeir, Robin Bonicel; CATI, Sorbonne Université; Institut du Cerveau - ICM, Assistance Publique Hôpitaux de Paris, Inserm, CNRS; Département de Neurologie and NS-PARK/FCRIN Network, CIC Neurosciences, Hôpital Pitié-Salpêtrière, Paris, France.

Driss Valérie, Verna Claudia; Department of Neuroradiology, Montpellier University Hospital Center, Gui de Chauliac Hospital, Montpellier, France.

Blard Fabrice, Dupouy Sandrine; Department of Neurology - Maladies Neurodégénératives, CHU Bordeaux, F-33000 Bordeaux, France.

Chatelain Anne; Department of Neurology, CHRU Nancy.

Bonnaire Margaux; Department of Neurology, Hôpital Maison blanche, Reims, France.

Boudjema Noel; Centre Expert Parkinson, CHU Henri Mondor, AP-HP et Equipe Neuropsychologie Interventionnelle, INSERM-IMRB, Faculté de Santé, Université Paris-Est Créteil et Ecole Normale Supérieure Paris Sorbonne Université.

Rabois Emilie; INSERM CIC-1402, Department of Neurology, CHU of Poitiers, University of Poitiers.

Rosique Pauline; Centre d'Investigation Clinique CIC 1436, UMR 1214 TONIC and NS-Park/FCRIN Network; INSERM, CHU of Toulouse, University of Toulouse3, Toulouse, France.

Appendix B. Supplementary data

Supplementary data to this article can be found online at https://doi.org/10.1016/j.nicl.2022.103231.

References

Arribarat, G.P., De Barros, A., Galitzky, M., Rascol, O., Péran, P., 2019. Substantia nigra locations of iron-content, free-water and mean diffusivity abnormalities in moderate stage Parkinson's disease. Parkinsonism Relat Disord 65, 146–152.

Ashburner, J., 2007. A fast diffeomorphic image registration algorithm. Neuroimage 38, 95–113.

Ashburner, J., Friston, K., 2005. Unified segmentation. Neuroimage 26 (3), 839–851.

Azuma, M., Hirai, T., Yamada, K., Yamashita, S., Ando, Y., Tateishi, M., al., 2016. Lateral asymmetry and spatial difference of iron deposition in the substantia nigra of patients with Parkinson disease measured with quantitative susceptibility mapping. AJNR Am J Neuroradiol 37, 782–788.

Barbosa, J.H., Santos, A.C., Tumas, V., Liu, M., Zheng, W., Haacke, E.M., al., 2015. Quantifying brain iron deposition in patients with Parkinson's disease using quantitative susceptibility mapping, R2 and R2. Magn Reson Imaging 33 (5), 559–565.

Baudrexel, S., Nürnberger, L., Rüb, U., Seifried, C., Klein, J.C., Deller, T., al., 2010. Quantitative mapping of T1 and T2* discloses nigral and brainstem pathology in early Parkinson's disease. Neuroimage 51 (2), 512–520.

Brammerloh, M., Weigelt, I., Arendt, T., Gavriilidis, F., Scherf, N., Jankuhn, S., al., 2018. Iron-induced relaxation mechanisms in the human substantia nigra: Towards quantifying iron load in dopaminergic neurons. ISMRM2018.

Brooks, D.L., Gadian, P., Marsden, D., Cd., 1989. Does signal-attenuation on high-field T2-weighted MRI of the brain reflect regional cerebral iron deposition? Observations on the relationship between regional cerebral water proton T2 values and iron levels. J Neurol Neurosurg Psychiatry 52 (1), 108–111.

Camlidag, I., Kocabicak, E., Sahin, B., Jahanshahi, A., Incesu, L., Aygun, D., al., 2014. Volumetric analysis of the subthalamic and red nuclei based on magnetic resonance imaging in patients with Parkinson's disease. International Journal of Neuroscience 124 (4), 291–295.

Castella, R., Arn, L., Dupuis, E., Callaghan, M.F., Draganski, B., Lutti, A., 2018. Controlling motion artefact levels in MR images by suspending data acquisition during periods of head motion. Magn Reson Med 80, 2415–2426.

Chaudhuri, K.H., Schapira, D., Ahv., 2006. The non-motor symptoms of Parkinson's disease. Diagnosis and management. *Lancet Neurol* 5, 235–245.

Chavhan, G.B.B., Thomas, P.S., Shroff, B., Haacke, M.M., E. m., 2009. Principles, techniques, and applications of T2*-based MR imaging and its special applications. Radiographics 29 (5), 1433–1449.

Cheng, Q., Huang, J., Liang, J., Ma, M., Zhao, Q., Lei, X., al., 2020. Evaluation of abnormal iron distribution in specific regions in the brains of patients with Parkinson's disease using quantitative susceptibility mapping and R2* mapping. Exp Ther Med 19 (6), 3778–3786.

Cohen, J. (1988). Statistical Power Analysis for the Behavioral Sciences (2nd ed.) (N. Hillsdale Ed.). New York: Lawrence Erlbaum Associates.

Colpan, M.E., Slavin, K.V., 2010. Subthalamic and red nucleus volumes in patients with Parkinson's disease: do they change with disease progression? Parkinsonism & Related Disorders 16 (6), 398–403.

Dexter, D., Wells, F., Lees, A., Agid, F., Agid, Y., Jenner, P., al., 1989. Increased nigral iron content and alterations in other metal ions occurring in brain in Parkinson's disease. J Neurochem 52, 1830–1836.

Du, G., Lewis, M.M., Styner, M., Shaffer, M.L., Sen, S., Yang, Q.X., al., 2011. Combined R2* and diffusion tensor imaging changes in the substantia nigra in Parkinson's disease. Mov Disord 26 (9), 1627–1632.

Du, G., Lewis, M., Sen, S., Wang, J., Shaffer, M., Styner, M., al., 2012. Imaging nigral pathology and clinical progression in Parkinson's disease. Mov Disord 27, 1636–1643.

Du, G., Lewis, M.M., Sica, C., He, L., Connor, J.R., Kong, L., al., 2018. Distinct progression pattern of susceptibility MRI in the substantia nigra of Parkinson's patients. Mov Disord 33 (9), 1423–1431.

Duvernoy, H. (1995). The human brain stem and cerebellum:Surface, Structure, Vascularization, and Three-Dimensional Sectional Anatomy, with MRI (Vol. 7): Springer-Verlag Wien.

Duyn, J.H.S.J., 2017. Contributions to magnetic susceptibility of brain tissue. NMR Biomed 30 (4).

Eapen, M.Z., Gatenby, D.H., Ding, J.C., Gore, Z., Jc., 2011. Using high-resolution MR imaging at 7T to evaluate the anatomy of the midbrain dopaminergic system. AJNR. Am J Neuroradiol 32 (4), 688–694.

Fernández-Seara, M.W.F.W., 2000. Postprocessing technique to correct for background gradients in image-based R2* measurements. Magn Reson Med 44, 358–366.

Gaurav, R., Yahia-Cherif, L., Pyatigorskaya, N., Mangone, G., Biondetti, E., Valabrègue, R., al., 2021. Longitudinal Changes in Neuromelanin MRI Signal in Parkinson's Disease: A Progression Marker. Mov Disord 36 (7), 1592–1602.

Gay, D., Chupin, M., Mangin, J., Poupon, C., Dary, H., Kaaouana, T., al., 2016. A standardised clinical multicentric whole brain T2* mapping protocol at 3T. Paper presented at the ISMRM Annual Meeting, Montréal.

Gelman, N., Gorell, J.M., Barker, P.B., Savage, R.M., Spickler, E.M., Windham, J.P., al., 1999. MR imaging of human brain at 3.0 T: preliminary report on transverse relaxation rates and relation to estimated iron content. Radiology 210 (3), 759–767.

Giladi, N., Tal, J., Azulay, T., Rascol, O., Brooks, D.J., Melamed, E., al., 2009. Validation of the freezing of gait questionnaire in patients with Parkinson's disease. Mov Disord 24 (5), 655–661.

Goetz, C.G., Tilley, B.C., Shaftman, S.R., Stebbins, G.T., Fahn, S., Martinez-Martin, P., al., 2008. Movement Disorder Society UPDRS Revision Task Force. Movement Disorder Society-sponsored revision of the Unified Parkinson's Disease Rating Scale (MDS-UPDRS): scale presentation and clinimetric testing results. Mov Disord 23 (15), 2129–2170.

Gorell, J.O., Brown, R.J., Deniau, G.G., Buderer, J.C., Helpern, N.M., Ja., 1995. Increased iron-related MRI contrast in the substantia nigra in Parkinson's disease. Neurology 45, 1138–1143.

Graham, J.M.P., Grunewald, M.N., Hoggard, R.A., Griffiths, N., P d., 2000. Brain iron deposition in Parkinson's disease imaged using the PRIME magnetic resonance sequence. Brain 123, 2423–2431.

Guan, X.X., Zhang, X., M., 2017. Region-Specific Iron Measured by MRI as a Biomarker for Parkinson's Disease. Neurosci Bull 33 (5), 561–567.

Hamilton, M., 1959. The assessment of anxiety states by rating. Br J Med Psychol 32, 50–55.

He, N., Ling, H., Ding, B., Huang, J., Zhang, Y., Zhang, Z., al., 2015. Region-specific disturbed iron distribution in early idiopathic Parkinson's disease measured by quantitative susceptibility mapping. Hum Brain Mapp 36 (11), 4407–4420.

Hedlund, J.L., Vieweg, B.W., 1979. The Hamilton rating scale for depression: a comprehensive review. J Oper Psychiatr 10 (2), 149–165.

Hoehn, M.M., Yahr, M.D., 1998. Parkinsonism: onset, progression, and mortality.1967. Neurology 50 (2), 318–334.

Hopes, L., Grolez, G., Moreau, C., Lopes, R., Ryckewaert, G., Carrière, N., al., 2016. Magnetic Resonance Imaging Features of the Nigrostriatal System: Biomarkers of Parkinson's Disease Stages? PLoS One 11 (4), e0147947.

Johns, M.W., 1991. A new method for measuring daytime sleepiness: the Epworth sleepiness scale. Sleep 14 (6), 540–545.

Kennan, R.Z., Gore, J.J.C., 1994. Intravascular susceptibility contrast mechanisms in tissues. Magn Reson Med 31 (1), 9–21.

Keuken, M., 2014. Quantifying inter-individual anatomical variability in the subcortex using 7 T structural MRI. Neuroimage 1 (94), 40–46.

Keuken, M.F., Bu, 2015. A probabilistic atlas of the basal ganglia using 7 T MRI. Data in Brief 577–582.

Kolpakwar, S., Arora, A.J., Pavan, S., Kandadai, R.M., Alugolu, R., al., 2021. Volumetric analysis of subthalamic nucleus and red nucleus in patients of advanced Parkinson's disease using SWI sequences. Surg Neurol Int 12 (377).

Langkammer, C., Krebs, N., Goessler, W., Scheurer, E., Ebner, F., Yen, K., al., 2010. Quantitative MR imaging of brain iron: a postmortem validation study. Radiology 257 (2), 455–462.

Langkammer, C., Pirpamer, L., Seiler, S., Deistung, A., Schweser, F., Franthal, S., al., 2016. Quantitative Susceptibility Mapping in Parkinson's Disease. PLoS One 11 (9).

Langley, J.H., Sedlacik, D.E., Boelmans, J., X. p., K., 2017. Parkinson's disease-related increase of T2*-weighted hypointensity in substantia nigra pars compacta. Mov Disord 32 (3), 441–449.

Lehéricy, S., Bardinet, E., Poupon, C., Vidailhet, M., François, C., 2014. 7 Tesla magnetic resonance imaging: a closer look at substantia nigra anatomy in Parkinson's disease. Mov Disord 29 (13), 1574–1581.

Lewis, M.M., Du, G., Kidacki, M., Patel, N., Shaffer, M.L., Mailman, R.B., al., 2013. Higher iron in the red nucleus marks Parkinson's dyskinesia. Neurobiol Aging 34 (5), 1497–1503.

Li, J., Chang, S., Liu, T., Wang, Q., Cui, D., Chen, X., al., 2012. Reducing the object orientation dependence of susceptibility effects in gradient echo MRI through quantitative susceptibility mapping. Magn Reson Med 68, 1563–1569.

Liu, Z., Li, Z., Qu, J., Zhang, R., Zhou, X., Li, L., al., 2019. Radiomics of Multiparametric MRI for Pretreatment Prediction of Pathologic Complete Response to Neoadjuvant Chemotherapy in Breast Cancer: A Multicenter Study. Clin Cancer Res 25 (12), 3538–3547.

Marek, K., Jennings, D., Lasch, S., Siderowf, A., Tannner, C., Simuni, T., al., 2011. The Parkinson Progression Marker Initiative (PPMI). Progress in Neurobiology 95, 629–635.

Martin, W.R.W., Gee, M., 2008. Midbrain iron content in early Parkinson disease: a potential biomarker of disease status. Neurology 70, 1411–1417.

Murakami, Y., Kakeda, S., Watanabe, K., Ueda, I., Ogasawara, A., Moriya, J., al., 2015. Usefulness of quantitative susceptibility mapping for the diagnosis of Parkinson disease. AJNR Am J Neuroradiol 36 (6), 1102–1108.

Nasreddine, Z.S., Phillips, N.A., Bédirian, V., Charbonneau, S., Whitehead, V., Collin, I., al., 2005. The Montreal Cognitive Assessment, MoCA: a brief screening tool for mild cognitive impairment. J Am Geriatr Soc 53 (4), 695–699.

Péran, P., Cherubini, A., Assogna, F., Piras, F., Quattrocchi, C., Peppe, A., al., 2010. Magnetic resonance imaging markers of Parkinson's disease nigrostriatal signature. Brain 133 (11), 3423–3433.

Postuma, R.B.B., Stern, D., M., 2015. MDS clinical diagnostic criteria for Parkinson's disease. Mov Disord 30 (12), 1591–1601.

Prensa, L., Parent, A., 2001. The nigrostriatal pathway in the rat: A single-axon study of the relationship between dorsal and ventral tier nigral neurons and the striosome/matrix striatal compartments. J Neurosci 21, 7247–7260.

Pyatigorskaya, N., Sharman, M., Corvol, J.C., Valabregue, R., Yahia-Cherif, L., Poupon, F., al., 2015. High nigral iron deposition in LRRK2 and Parkin mutation carriers using R2* relaxometry. Mov Disord 30 (8), 1077–1084.

Pyatigorskaya, N., Sanz-Morère, C.B., Gaurav, R., Biondetti, E., Valabregue, R., Santin, M., al., 2020. Iron Imaging as a Diagnostic Tool for Parkinson's Disease: A Systematic Review and Meta-Analysis. Front Neurol 11, 366.

Reimão, S., Pita Lobo, P., Neutel, D., Correia Guedes, L., Coelho, M., Rosa, M.M., al., 2015. Substantia nigra neuromelanin magnetic resonance imaging in de novo Parkinson's disease patients. Eur J Neurol 22 (3), 540–546.

Riederer, P., Sofic, E., Rausch, W., Schmidt, B., Reynolds, G., Jellinger, K., al., 1989. Transition metals, ferritin, glutathione, and ascorbic acid in parkinsonian brains. J Neurochem 52 (2), 515–520.

Rieu, I., Martinez-Martin, P., Pereira, B., De Chazeron, I., Verhagen Metman, L., Jahanshahi, M., al., 2015. International validation of a behavioral scale in Parkinson's disease without dementia. Mov Disord 30 (5), 705–713.

Rossi, M.E.R., Saunamäki, H., Elovaara, T., Dastidar, I., P., 2014. Imaging brain iron and diffusion patterns: a follow-up study of Parkinson's disease in the initial stages. Acad Radiol 21 (1), 64–71.

Russek, S., Boss, M., Jackson, E., Jennings, D., Evelhoch, J., Gunter, J., & al. (2012). Characterization of NIST/ISMRM MRI system phantom. Paper presented at the ISMRM.

Schenck, J.F., 1995. Imaging of brain iron by magnetic resonance: T2 relaxation at different field strengths. J Neurol Sci 134.

Schwab, R.S., 1960. Progression and prognosis in Parkinson's disease. Journal of Nervous and Mental Disease 130, 556–566.

Sethi, S.K., Kisch, S.J., Ghassaban, K., Rajput, A., Rajput, A., al., 2019. Iron quantification in Parkinson's disease using an age-based threshold on susceptibility maps: The advantage of local versus entire structure iron content measurements. Magn Reson Imaging 55, 145–152.

Shah, A.S., Sylvester, P.T., Yahanda, A.T., Vellimana, A.K., Dunn, G.P., Evans, J., al., 2020. Intraoperative MRI for newly diagnosed supratentorial glioblastoma: a multicenter-registry comparative study to conventional surgery. J Neurosurg 1–10.

Sockeel, P.D., Devos, K., Denève, D., Destée, C., Defebvre, A., L., 2006. The Lille apathy rating scale (LARS), a new instrument for detecting and quantifying apathy: validation in Parkinson's disease. J Neurol Neurosurg Psychiatry 77 (5), 579–584.

Stüber, C.P., Wang, D.Y., 2016. Iron in Multiple Sclerosis and Its Noninvasive Imaging with Quantitative Susceptibility Mapping. Int J Mol Sci 17 (1).

Tomlinson, C.S., Patel, R., Rick, S., Gray, C., Clarke, R., Ce., 2010. Systematic review of levodopa dose equivalency reporting in Parkinson's disease. Mov. Disord 25, 2649–2653.

Tosk, J., Holshouser, B., Aloia, R., Hinshaw, D., Hasso, A., MacMurray, J., al., 1992. Effects of the interaction between ferric iron and L-dopa melanin on T1 and T2 relaxation times determined by magnetic resonance imaging. Magn Reson Med 26 (1), 40–45.

Tremblay, L.W., Thobois, Y., Sgambato-Faure, S., Féger, V., J., 2015. Selective dysfunction of basal ganglia subterritories: From movement to behavioral disorders. Mov Disord 30 (9), 1155–1170.

Trujillo, P., Summers, P., Ferrari, E., Zucca, F., Sturini, M., Mainardi, L., al., 2017. Contrast mechanisms associated with neuromelanin-MRI. Magn Reson Med 78 (5), 1790–1800.

Ulla, M.B., Ouchchane, J.M., Rieu, L., Claise, I., Durif, B., F., 2013. Is R2* a new MRI biomarker for the progression of Parkinson's disease? A longitudinal follow-up. *PLoS One* 8 (3), e57904.

Visser, M.M., Stiggelbout, J., Van Hilten, A.M., Jj., 2004. Assessment of autonomic dysfunction in Parkinson's disease: the SCOPA-AUT. Mov Disord 19 (11), 1306–1312.

Wallis, L.I., Paley, M.N., Graham, J.M., Grünewald, R.A., Wignall, E.L., Joy, H.M., al., 2008. MRI assessment of basal ganglia iron deposition in Parkinson's disease. J Magn Reson Imaging 28 (5), 1061–1067.

Wei, W., Wang, X., 2016. Inhibitory Control in the Cortico-Basal Ganglia-Thalamocortical Loop: Complex Regulation and Interplay with Memory and Decision Processes. Neuron 92 (5), 1093–1105.

Wieler, M.G., Martin, M., W. r., 2015. Longitudinal midbrain changes in early Parkinson's disease: iron content estimated from R2*/MRI. Parkinsonism Relat Disord 21 (3), 179–183.

Wolozin, B., Golts, N., 2002. Iron and Parkinson's Disease. The Neuroscientist 8 (1), 22–32.

Yablonskiy, D.A., Haacke, E.M., 1994. Theory of NMR signal behavior in magnetically inhomogeneous tissues: the static dephasing regime. Magn Reson Med 32 (6), 749–763.

Yushkevich, P., Piven, J., Hazlett, H., Smith, R., Ho, S., Gee, J., al., 2006. User-guided 3D active contour segmentation of anatomical structures: Significantly improved efficiency and reliability. Neuroimage 31 (3), 1116–1128.

Further reading

Wang, J., Zhuang, Q., Zhu, L., Zhu, H., Li, T., Li, R., al., 2016. Meta-analysis of brain iron levels of Parkinson's disease patients determined by postmortem and MRI measurements. Sci Rep 6, 36669.